

# Variability of rainy season onsets over East Africa

Emmah Mwangi<sup>1</sup>  | Dave MacLeod<sup>2</sup> | Dominic Kniveton<sup>1</sup> | Martin C. Todd<sup>1</sup>

<sup>1</sup>Department of Geography, University of Sussex, Brighton, UK

<sup>2</sup>University of Cardiff, Cardiff, UK

## Correspondence

Emmah Mwangi, Department of Geography, University of Sussex, Sussex House, Falmer, Brighton BN1 9RH, UK.  
Email: [e.mwangi@sussex.ac.uk](mailto:e.mwangi@sussex.ac.uk)

## Funding information

Science for Humanitarian Emergencies and Resilience (SHEAR) consortium project, Grant/Award Numbers: NE/P000673/1, NE/P000568/1, NE/P000428/1, NE/P000444/1; Sussex University Scholarship programme

## Abstract

Over the East Africa region forecasts of the onset of the rainy seasons have the potential to support decision-making, especially in the largely rain-fed agricultural sector. However, the understanding of key features of onset remains limited. Here, we analyse the variability of onset and associated drivers at interannual and subseasonal timescales, using several onset definitions. Results show that the onset date is especially variable from year to year in some of the high-potential agricultural areas (standard deviation >20 days), which has implications for agricultural risk management. The choice of onset definition metric matters; agronomic definitions have limited applicability at the regional scale and are also highly sensitive to the spatial scale of analysis and to the choice of rainfall data. Onset information provided at coarse scales should be used with caution for decision-making at the local scale; the “hit rate” of coarse-scale tercile onset information at the local scale is less than 40% on average. To varying degrees, onset is related to total seasonal rainfall and thus to dominant interannual drivers of rainfall, including the Indian Ocean Dipole and ENSO modes in October–December and the western Pacific “V-gradient” pattern in March–May. However, by analysing the dominant proportion of onset variance unrelated to total rainfall during the climatological season we show a substantial influence of subseasonal drivers, notably the Madden–Julian Oscillation. As such, there is an opportunity for rainfall onset information to be provided across seasonal and subseasonal timescales. Our work reinforces the need for enhanced co-production of such onset information with stakeholders, especially regarding the choice of metric, alignment of forecasts with livelihood calendars, interpretation of the credibility of information content for local-level decision-making, as well as appropriate strategies for staggered risk management interventions informed by forecasts over “seamless” lead times.

## KEYWORDS

co-production, East Africa, Madden–Julian Oscillation, onset, onset definition, subseasonal

This is an open access article under the terms of the [Creative Commons Attribution](https://creativecommons.org/licenses/by/4.0/) License, which permits use, distribution and reproduction in any medium, provided the original work is properly cited.

© 2024 The Authors. *International Journal of Climatology* published by John Wiley & Sons Ltd on behalf of Royal Meteorological Society.

## 1 | INTRODUCTION

In East Africa (EA), livelihoods, food security and indeed gross domestic product (GDP) are substantially dependent on rain-fed agricultural production (Kadi et al. 2011) and thus are highly vulnerable to climate variability and change. For a recent broad review of EA climate variability and trends and the societal impacts, see Palmer et al. (2023). Actionable climate information can support more optimal agricultural decisions. Forecasts of the timing of the seasonal rain onset are often ranked by users as the most important metric (Owusu et al., 2017; UK Met Office, 2011). Accurate knowledge of the onset date can boost yield by reducing the risk of planting late or early (Laux et al., 2008) by guiding the implementation of key cropping decisions such as land preparation, purchase of inputs, sowing dates, mobilization of manpower and equipment (Acharya & Bennett, 2021). For example, the delayed onset of March–May (MAM) rains in 2019 was associated with a 20% reduction in total maize production in Kenya (Global Agricultural Monitoring, 2019). “False onsets” in which a prolonged dry spell occurs shortly after an initial wet spell, can lead to seedling death and the need for replanting (Gbangou et al., 2019) as in Western Kenya in MAM 2019 (Feed the Future, 2019). Currently, climate information services in the EA region have a dominant focus on forecasts of seasonal rainfall totals, although forecasts of onset date are also provided (e.g., <https://www.icpac.net/seasonal-forecast/>). Notably, an opportunity exists for advancing forecast information in EA given the relatively high predictability of climate across seasonal to subseasonal time-scales (de Andrade et al., 2019; MacLeod et al., 2021; Walker et al., 2019).

Based on the multiscale nature of rainfall variability, defining the onset of the rainy season is complex and further should depend on the intended application. Over 20 onset definitions have been published for the West African monsoon (Fitzpatrick et al., 2015). While onset can be defined using a combination of atmospheric circulation parameters, most definitions are based on rainfall only, due to the availability of historical rainfall data—compared to other parameters such as soil moisture—and the direct relevance to agricultural practices (Ferijal et al., 2022). “Agronomic” onset definitions are typically based on point-scale rainfall exceeding some threshold of accumulated rainfall, deemed sufficient for seed germination but with an added condition to avoid false onset, that is, no significant dry spell in the subsequent days (Acharya & Bennett, 2021; Laux et al., 2008; Marteau et al., 2009; Stern et al., 1981). Forecasting centres in EA such as the IGAD Climate Prediction and Applications Centre (ICPAC) operationally utilize agronomic definitions (Table 1) across the entire region/country.

However, such definitions are problematic when applied over large areas or using relatively coarse observations because (i) the rainfall thresholds usually established from point scale studies may not apply to spatially averaged rainfall information (ii) cropping patterns and thus water requirements likely differ over large regions such that crop-relevant thresholds may not be appropriate. Such problems can be addressed using definitions based on the accumulated daily anomalies with respect to the local mean (Camberlin & Okoola, 2003; Dunning et al., 2016; MacLeod, 2018).

To date, no assessment of the applicability of operational or other onset definitions has been conducted for EA. This is despite studies over other regions such as West Africa showing strong sensitivity of the mean onset date, onset variability, onset drivers, and thus likely forecast skill to onset definitions (Fitzpatrick et al., 2015; Vellinga et al., 2013). Further, scientific literature on EA rainfall has mainly focused on understanding the seasonality, variability and drivers of total seasonal rainfall. EA has a complex seasonality (Herrmann & Mohr, 2011; Liebmann et al., 2017) which has been associated with EA’s topography and location astride the equator. Herrmann and Mohr (2011) show pronounced spatial gradients in seasonality regimes in close spatial proximity such that in Western Kenya and Northern Uganda, there exist up to five different seasonality regimes. The role of IOD and ENSO in driving OND rainfall variability is well established (Black, 2005; Indeje et al., 2000; Marchant et al., 2007; Mutai & Ward, 2000; Ogallo, 1988). The MAM season is generally believed to be less strongly associated with tropical modes and has weaker predictability (Walker et al., 2019), although in recent decades the role of the Pacific Ocean temperatures in driving dry MAM conditions (Funk et al., 2015) and the Madden–Julian Oscillation (MJO) activity (Maybee et al., 2022) has emerged. There has been a recent focus on subseasonal variability indicating relatively strong predictability at these time-scales linked to improvement in the representation of the MJO (Finney et al., 2020; MacLeod et al., 2021). However, there has been little focus on how these systems influence onset variability, despite the ongoing operational provision of onset forecasts.

Those studies that have focused on drivers of onset variability have been conducted over large scales or one part of the East African region with each study utilizing one onset definition (detailed in Table 1). Various studies have linked the variability of onset in MAM to the atmospheric response to patterns of sea surface temperature (SST) including the SST gradient between the Atlantic and Indian Oceans (Camberlin & Okoola, 2003); The South Indian Ocean (Wainwright et al., 2019); The Western Pacific “V” shape region (Funk et al., 2023). In the

**TABLE 1** Onset definitions that are documented and operationally used over the East African region.

Onset metric category	Reference	Onset definition
Accumulated daily anomalies	Dunning et al. (2016)	Referred to as onset metric AA in this study. Inspired by Liebmann and Marengo (2001), defines onset as the minima in the cumulative daily precipitation anomaly. The onset date at the grid point level is defined as the minima of the accumulated daily rainfall anomalies time series with the anomalies calculated relative to the long-term mean of a rainy season
	Camberlin and Okoola (2003)	(Not used in this study) Inspired by Liebmann and Marengo (2001). The onset date was defined as the minima of the accumulated principal component (PC) time series of the leading mode of the daily station rainfall empirical orthogonal function (EOF) analysis over Kenya and Northern Tanzania
Agronomic: threshold of accumulated daily rainfall	IGAD Climate Prediction and Applications Centre (ICPAC) (Gudoshava et al., 2022)	Referred to as onset metric AG1 in this study. Adopted as the operational onset definition at the IGAD Climate Prediction Centre over the Greater Horn of Africa (ICPAC). Onset is the first day of the wet season when a wet spell of accumulated rainfall in 3 consecutive days is 20 mm and there is no dry spell of over 7 days in the next 20 days. The threshold for a rainy day is defined as 1 mm
	Kijazi and Reason (2012)	Referred to as onset metric AG2 in this study. The first wet day of a 5-day period whose accumulated rainfall exceeds 10 mm followed by three consecutive pentads having a rainfall amount of not less than 10 mm per pentad
	Kenya Meteorological Department (KMD)	(Not used in this study) Utilizes the same definition as ICPAC. However, for the arid and semi-arid areas (ASALs) the accumulated threshold is lowered to 10 mm

OND season onset variability links most strongly to circulation anomalies associated with the Indian Ocean Dipole (Gudoshava et al., 2022a). However, such interannual variability explains only a relatively small proportion of onset variance (up to around 50%; MacLeod, 2018) such that subseasonal and higher frequency synoptic scale variability is crucial. Given that onset is fundamentally a relatively short-term phenomenon but is influenced by longer-term structures of variability there is a need for greater clarity on how climate/weather drivers that operate across space/time scales interact to determine onset variability.

Such improved understanding of drivers of onset and the sensitivity to onset metric definition across multiple scales of analysis is important for informing the development and use of appropriate products for agricultural planning and risk management. In this study, we address the following research questions.

1. What is the spatial and temporal nature of onset variability across the East African region?

2. How sensitive are onset characteristics to the choice of onset metric and scale of analysis?
3. What are the key drivers of variability in onset across interannual to subseasonal timescales?

## 2 | DATA AND METHODS

### 2.1 | Rainfall

The primary precipitation dataset used is the Climate Hazards Group Infrared Precipitation with Stations (CHIRPS) from 1981 to 2020, available at daily/0.05° resolution. CHIRPS blends gauge data with rainfall calculated from thermal infrared satellite imagery (Funk et al., 2015) and performs well over East Africa (Kimani et al., 2017). However, to analyse the sensitivity of onset dates to different equally valid datasets, we also utilized daily Multi-Source Weighted-Ensemble Precipitation (MSWEP) at daily/0.1° resolution. MSWEP merges gauge, satellite, and reanalysis data (Beck et al., 2019) and is

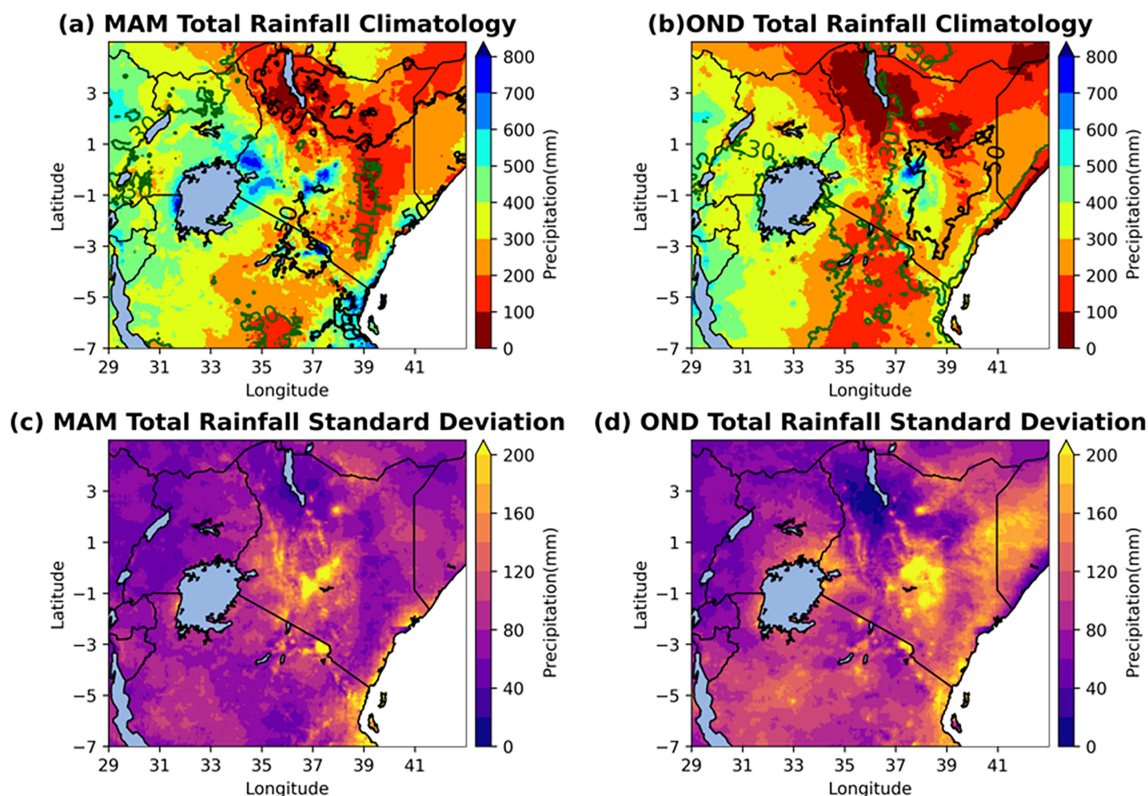


**FIGURE 1** (a, b) Seasonal mean rainfall (mm) for MAM and OND, respectively. (c, d) Standard deviation of seasonal rainfall (mm) for MAM and OND, respectively. Contours in (a, b) indicate the percentage contribution of the season to the annual total rainfall.

second to CHIRPS in performance over parts of EA (Omonge et al., 2022).

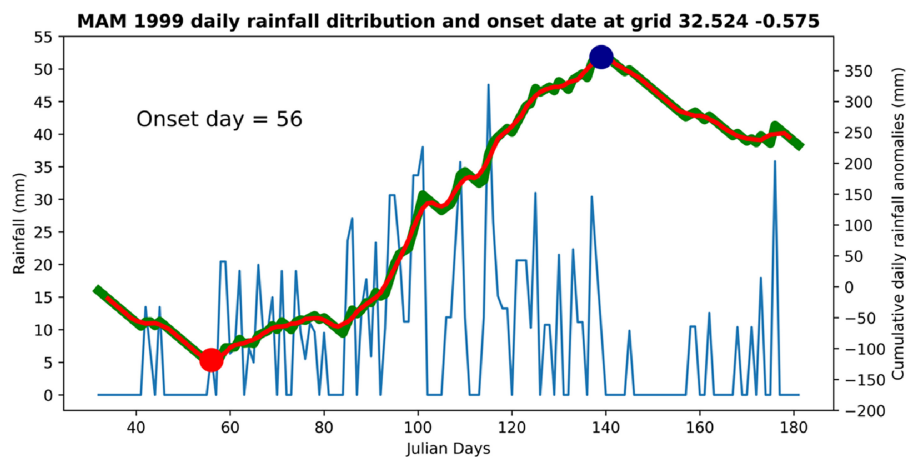
We assess rainfall onset over a domain covering equatorial EA bounded by 7°S and 5°N; 29°E and 43°E comprising Kenya, Uganda, Northern Tanzania, Rwanda, Burundi, Southern Somalia, Southern Ethiopia and Southern South Sudan (Figure 1). Although most of the region receives rainfall during two main seasons: the “long rains” season from March to May (MAM) and the “short rains” season from October to December (OND), the seasonality of rainfall over the region is much more complex.

The Eastern sector ( $\sim 37^{\circ}$ – $42^{\circ}$ E) of the region exhibits two distinct seasons while the extreme South ( $<5^{\circ}$ S) has one season, as illustrated in Figures S1 and S2, Supporting Information. This is corroborated by previous studies (Dunning et al., 2016; Herrmann & Mohr, 2011; Liebmann et al., 2017). However, the characterization of seasonality in parts of Uganda and Western Kenya (WKNU) varies depending upon the methodology employed and the rainfall dataset used. Using harmonic analysis of the local rainfall climatology, Dunning et al. (2016) delineate two seasons across equatorial East Africa, while Liebmann et al. (2017) identify two seasons

in much of Uganda and the Lake Victoria basin and unimodal seasonality in WKNU. Further, Herrmann and Mohr (2011) using a water balance methodology combining temperature and rainfall, highlight a more complex seasonality over WKNU, encompassing one wet season, two wet seasons and non-seasonal patterns, with unimodal and bimodality within the wet seasons. There are pronounced spatial gradients in regimes in close spatial proximity such that in WKNU there exist up to five different regimes. Further, they note the stability of the defined seasonality is very low in WKNU, that is, there is high interannual variability in seasonality.

Detailed agricultural livelihood calendars (available only for Kenya) from the Famine Early Warning Systems Network (FEWSNET) illustrate the complexity of agro-climate seasonality in Western Kenya (FEWSNET, 2011). Considering the transition from Lake Victoria to the Rift, there is a variation from zones with one to two maize-growing seasons which are associated with rainfall seasonality. The complex seasonality is further illustrated by time-longitude plot of mean daily rainfall, between latitudes 0° and 1°N which indicates one long rainfall season in Western Kenya and two slightly distinct rain seasons in central Uganda (Figure S1).

**FIGURE 2** Example of onset derivation using the AA onset metric for March to May 1999 at grid point 32.524°E, 0.575°S with onset indicated by the red dot. Plot shows daily rainfall (mm, blue line) with the cumulative daily rainfall anomalies (mm, green), and smoothed cumulative daily anomalies (mm, red). The red (dark blue) dots indicate the absolute minima (maxima) of the smoothed cumulative curve.



Due to the region's complex seasonality particularly the presence and duration of the second season over the western sector of EA, applying a single rule to seasonality in the region is difficult. Thus we consider the two seasons (MAM and OND) that are experienced over much of EA. Rainfall variability in these seasons is most pronounced over Kenya (Figure 1c) especially over central Kenya and Rift Valley, which are also Kenya's most agriculturally productive regions (USDA, 2009).

## 2.2 | Definition of onset

We utilize three definitions from Table 1 that are applicable for grid cell/localized analysis. Two are agronomic definitions (i) ICPAC's operational definition (ii) from Kijazi and Reason (2012) (hereafter, AG1 and AG2, respectively). The third definition is based on accumulated daily rainfall anomalies (hereafter, AA) from Dunning et al. (2016), with the onset being the transition from dry to wet, defined as the point of upturn in accumulated rainfall anomalies (averaged over 5 days), which are negative during dry periods but become positive when the rainfall first exceeds the daily norm. A typical case of AA is shown in Figure 2 with the onset date indicated by the red dot. The method was refined to cope with specific circumstances as described in sect. S1 and Figure S3.

Due to the region's complex seasonality, particularly the presence and duration of the second season over the Western sector of EA, we conducted onset sensitivity analysis for this season using different season lengths; July–December (JASOND); August–December (ASOND) and September–December (SOND). Further, acknowledging the absence of a perfect method for defining seasons due to complex seasonality and thus onsets, we implement several restrictions in our analysis: (i) we focus on seasons centred on February to May and

September to December, and (ii) we mask out areas that climatologically experience onsets before 1st March and 1st October. These restrictions are applied across the three definitions and climatological masks are unique for each definition.

## 2.3 | Spatial-temporal characterization of onset

We utilized empirical orthogonal function (EOF) analysis to determine the dominant spatial patterns of onset variability. Results over the domain of interest were essentially insensitive to the use of a larger domain of 10°S–7°N and 25°–45°E (Figures S4 and S5). We also assess the dependence of onset timing to the spatial scale of analysis by comparing onset dates at contrasting spatial resolutions (following Young et al., 2020), of the highest available resolution (0.05°), indicative of local scale decision-making, and a degraded coarse resolution of 1.0°, indicative of some of the available forecast products, e.g., the World Climate Research Programme/WMO S2S real-time pilot (<http://www.s2sprediction.net/>) provided forecast information degraded to 1.5°. We conduct this scale-dependence analysis by (i) deriving the temporal correlation of onset dates derived at fine and coarse resolution; (ii) deriving the “hit rate” at the fine scale of coarse scale, as the percentage of seasons that are in the same tercile category at both resolutions. This is analogous to a baseline assessment of the “skill” of a “perfect” onset forecast provided at low resolution assessed at the local-level more relevant to decision-making on the ground.

## 2.4 | Drivers of onset variability

We consider both interannual and intraseasonal controls on onset timing. At interannual timescales, we correlate

the EOF PCs (section 2.3) with SSTs from the National Oceanic and Atmospheric Administration's (NOAA) second version Optimum Interpolation (OI) monthly dataset (Reynolds et al., 2002). We focus on indices of relevant modes of variability of the Indian Ocean Dipole (IOD) and the recently defined "Western V Gradient (WVG)" in the Pacific. The IOD Index (DMI) was calculated as the difference between monthly SST anomalies in the western (50°–70°E, 10°S–10°N) and eastern (90°–110°E, 10°S–0°) Indian Ocean (Saji et al., 1999). The WVG (Funk et al., 2023) was computed as the difference between standardized SSTs over the NINO3.4 region (170°–120°W, 5°S–5°N) and the Western "V"; that is the averaged over West Pacific 120°–160°E, 15°S–20°N, Western North Pacific 160°E–150°W, 20°–35°N and Western South Pacific 155°E–150°W, 15°–30°S.

Distinguishing the interannual and intraseasonal influences on onset is not simple since the singular seasonal onset values are not amenable to standard time filtering. There is a well-documented observed association between seasonal total rainfall and onset dates, in which high (low) seasonal total rainfall results in earlier (delayed) onset (Camberlin & Okoola, 2003; Gudoshava et al., 2022a, 2022b; Kijazi & Reason, 2012; MacLeod, 2018). We assume that this association broadly reflects the interannual control on onset. This correlation, however, only explains at most about 50% of the variance in onset. Thus, to assess subseasonal influences we identify seasons when the association between rainfall onset and the rainfall total is relatively weak, for example, late-onset seasons which are not notably drier than normal or early-onset seasons that are not notably wetter than normal. We term these seasons, "deviant" seasons in the sense that onset timing deviates from that expected from the influence of interannual controls, and we then investigate the subseasonal drivers.

"Deviant" seasons at each grid cell are identified from the residuals of the linear regression of onset date and total rainfall during the climatological season (MAM and OND) across the study period (for the grid points with a statistically significant correlation; see, e.g., Figure S6). The major early and late "deviant" seasons were defined as those with the greatest areal coverage of grid cells with large residual values (below or above, respectively the 20th and 80th percentile of the residual distribution) across the three onset definitions. For each season category (early/late onset) we identified two seasons that have the largest percentage area across the three onset definitions. We caveat this methodology by recognizing that the residual of the regression is a simple method of separating interannual and subseasonal drivers and some of the deviation may well be from seasonal characteristics that are not linked to total seasonal

rainfall. However, this is a good starting point for exploring the deviance from the total seasonal rainfall and onset association.

For these major "deviant" seasons analysis of subseasonal drivers focused on the MJO, moisture convergence and wind flow. We utilize hourly 30-km spatial resolution 850 hPa zonal winds and vertically integrated moisture divergence from the fifth generation of European Centre for Medium-Range Weather Forecasts (ECMWF, ERA5) to analyse atmospheric conditions during onset. We use the Real-time Multivariate MJO (RMM; Wheeler & Hendon, 2004) to characterize the MJO phase and amplitude before, during, and after onset dates. The RMM is computed from the first two principal components (referred to as RMM1 and RMM2) of the ENSO signal-filtered analysis of combined daily global tropical outgoing longwave radiation (OLR) and NCEP-NCAR reanalysis zonal winds at 850 and 200 hPa. RMM1 and RMM2 form a two-dimensional Cartesian phase diagram that depicts the propagation of the MJO convective clusters eastwards across the Tropics. Figures S7 and S8 show the effect of MJO phases on rainfall across EA indicating that enhanced rainfall over EA is associated with MJO phases 2–4 (and to some extent phase 1), while suppressed rainfall over EA is associated with MJO phases 5–8.

## 3 | RESULTS AND DISCUSSION

### 3.1 | Nature of onsets across different onset definitions

Here we address research questions 1 and 2 with sections 3.1.1–3.1.3, respectively, presenting an assessment of the spatial patterns of the mean onset date and variability, the association between onset definition definitions, and the sensitivity of onset to the spatial scale of analysis and different rainfall datasets.

#### 3.1.1 | Patterns of mean wet season onset and variability

Mean rainfall onset date patterns broadly indicate the progression of onset from southwest to northwest across the domain during MAM (Figure 3a–c) and northwest to southeast during OND (Figure 3g–i). These patterns are consistent with earlier studies on the region (Camberlin & Okoola, 2003; Dunning et al., 2016; MacLeod, 2018; Gudoshava et al., 2022a, 2022b) and align with the customary explanation of the rainy seasons over East Africa being associated with the movement of the tropical rain

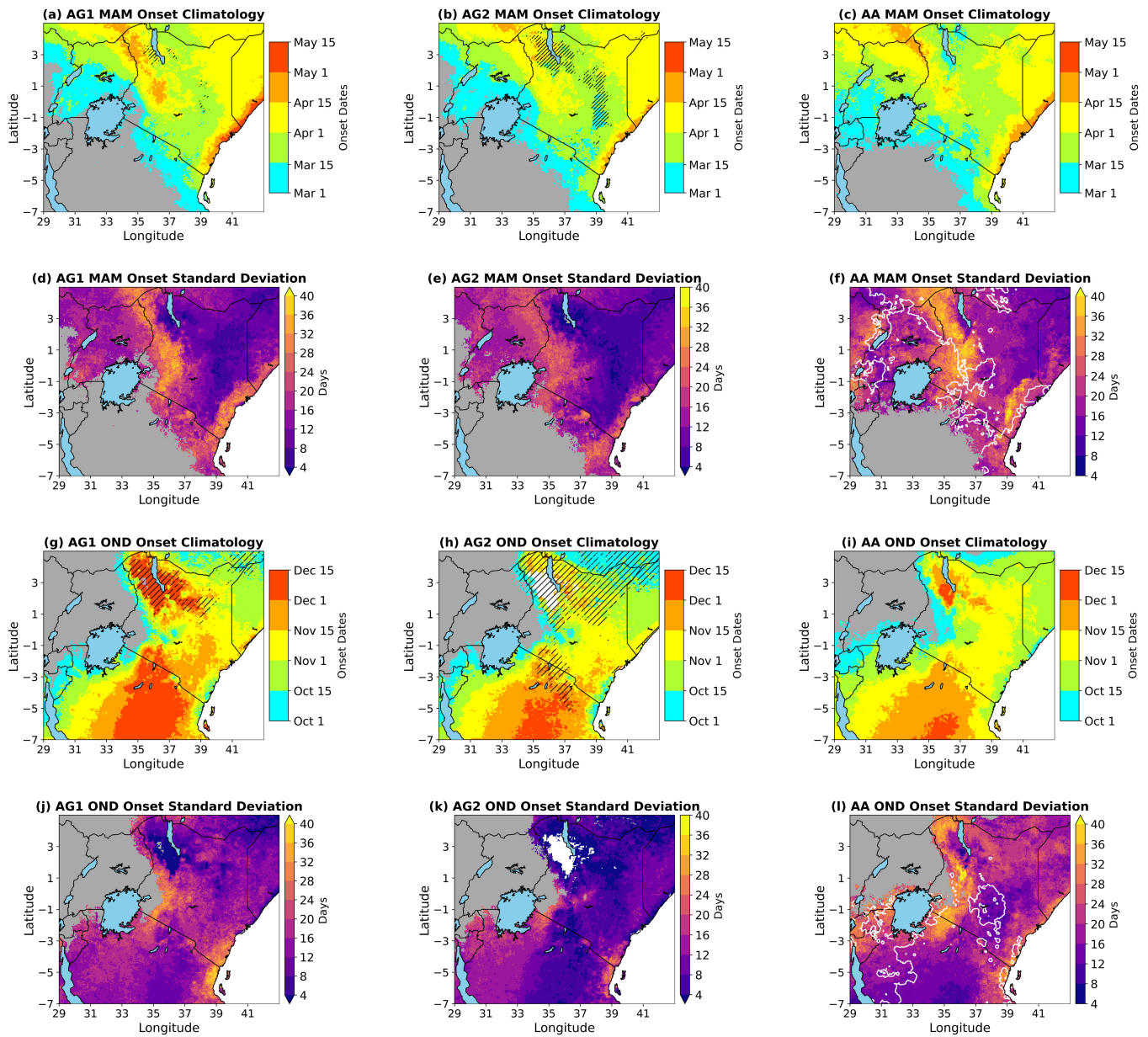


**FIGURE 3** Climatological onset dates for; (a–c) MAM and (g–i) OND, for the AG1, AG2 and AA onset definitions, respectively. (d–f) Temporal standard deviation of onset dates (days) for MAM and (j–l) for OND for definitions AG1, AG2 and AA, respectively. The white contours in (f, l) indicate areas that receive total rainfall of over 350 mm on average. Areas where the onset occurs before March 1st and October 1st for MAM and OND, respectively, are shown in grey. Hatching represents areas where less than 20% of the years attain an onset date.

**TABLE 2** Spatial correlation of the climatological onset dates and standard deviation across the three definitions for MAM and OND seasons.

	Spatial correlation of climatological onset dates		Spatial correlation of standard deviation	
	MAM	OND	MAM	OND
AG1 vs. AG2	0.92	0.90	0.76	0.64
AG1 vs. AA	0.74	0.78	0.63	0.33
AG2 vs. AA	0.75	0.84	0.45	0.21

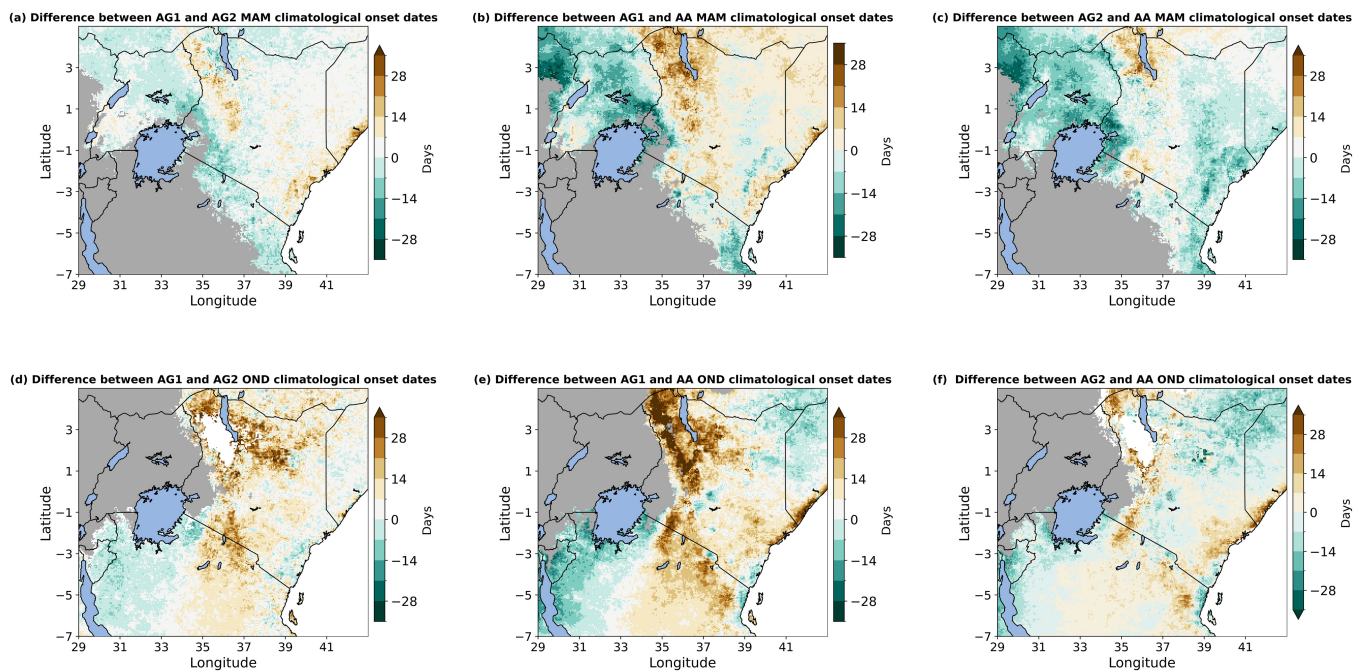


**FIGURE 4** Absolute differences in climatological mean onset dates (in days) between the three onset definitions. Difference between MAM onsets for (a) AG1 and AG2 (b) AG1 and AA (c) AG2 and AA. Difference between OND onsets for (d) AG1 and AG2 (e) AG1 and AA (f) AG2 and AA.

belt northwards and southwards, respectively. These basic patterns are consistent for all three onset definitions, confirmed by high spatial correlations of mean onset between definitions, especially in OND (Table 2). Note that the agronomic AG2 metric fails to achieve onset dates during any of the 40 years in OND in the arid Turkana region in the extreme northwest of Kenya.

However, absolute differences in mean onset between definitions locally are often high, exceeding 14 days in many places (Figure 4), presumably reflecting sensitivity to the different thresholds of rainfall accumulation and subsequent dry spells (Table 1) and the use of relative versus absolute rainfall. While the agronomic definitions arguably have greater relevance to practical applications in agriculture the pattern of mean onset for a given metric and its relevance to decision-making must be well understood and communicated (see section 3.1.3).

Perhaps of greater importance note is the magnitude of interannual variability in onset dates (Figure 3d–f,j–l) which varies markedly across the domain with the highest variability (>28 days) occurring in Kenya, especially over parts of the Coastal strip, Rift Valley and Western Kenya for both seasons. Rift Valley and Western Kenya are wetter areas of high agricultural production such that high onset variability likely has important implications for agricultural practices and affirms the potential importance of reliable onset information to inform decision-making and risk management. Note that the high onset

variability in these regions of Kenya contrasts with much lower variability over similarly humid regions in western Tanzania or Uganda. Agreement between the onset definitions in the spatial structure of variability is weaker than for mean onset (Table 2). Further, the spatial pattern of onset variability does not match especially closely with that of seasonal total rainfall variability (Figure 1c,d). This suggests that the drivers of onset and total rainfall variability may have significant differences (see section 3.2).

Sensitivity analysis for the second season indicates that onset dates shift with changes in season definition, and this is especially so for AG onset definitions (Figure S9). Notably, interannual variability in onset dates remains high over parts of the Coastal strip, Rift Valley and Western Kenya (Figure S9 d–f,j–l). The high variability over the Rift Valley and Western Kenya can be associated with the high interannual variability in seasonality that is noted by Herrmann and Mohr (2011).

### 3.1.2 | Association between onset definition definitions

Although mean onset patterns are very similar across onset definitions, the temporal association among them is low in many areas (Figure 5). However, a strong association is noted between AG1 and AG2 in the MAM season (Figure 5a). Not surprisingly, AA has a lower association

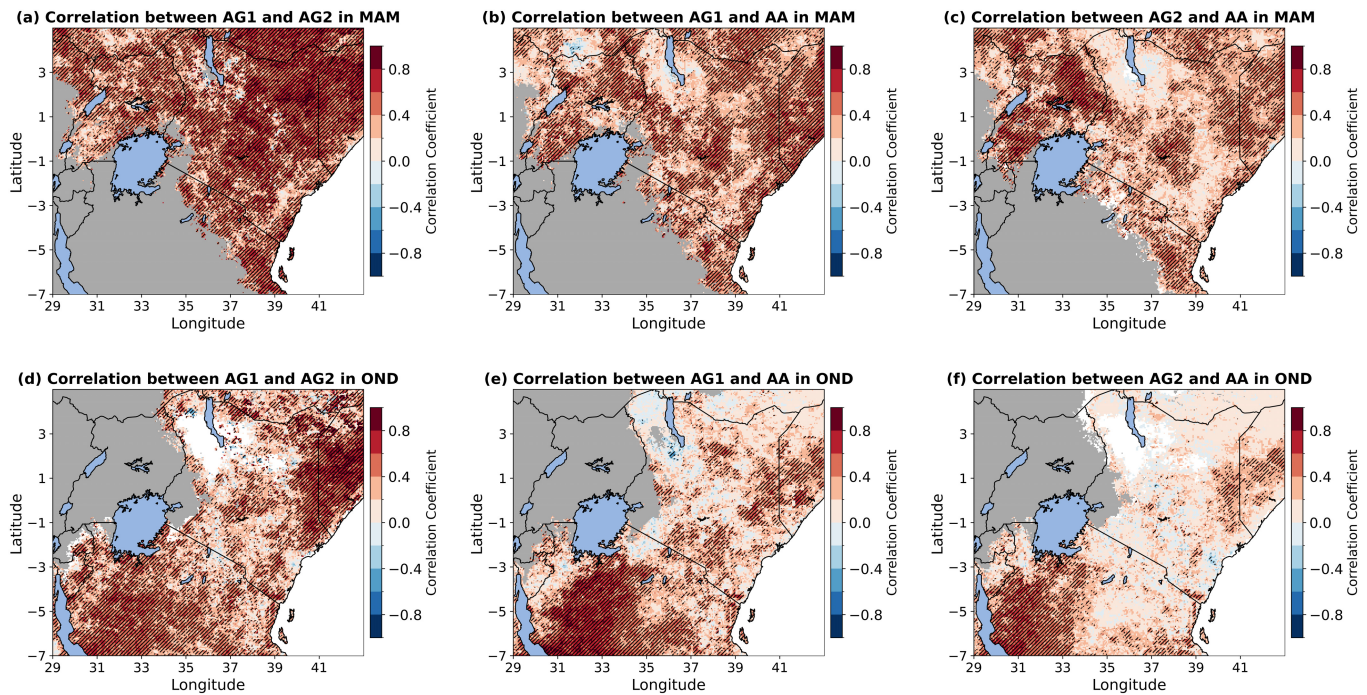


**FIGURE 5** Temporal correlation between onset dates across the period 1981–2020 from the three definitions; (a–c) MAM season and (d–f) OND season. Hatching represents correlations that are statistically significant at the 95% significance level.

with AG2 and AG1 with correlations less than 0.6 over much of the region. The association is weak, especially in OND (Figure 5f), for which there are large areas with nonsignificant correlations. This weak temporal agreement in onset among the definitions strongly indicates that the choice of onset metric is important in an operational context and should be considered carefully when assessing the predictability of onset forecasts.

### 3.1.3 | Sensitivity of onset to spatial resolution and different datasets

Typically, weather and climate information provided by meteorological services over EA is provided at spatial scales much coarser than that of local level decision making in agricultural management. Accordingly, we sought to investigate the sensitivity of onset dates to spatial scale. The temporal correlation of onset dates at fine ( $0.05^\circ$ ) and coarse resolution ( $1^\circ$ ) for the AA metric is very variable but generally quite strong ( $r > 0.6$ ) over much of the domain in both seasons (Figure 6i,j), although the correlation is lower in many areas especially where variability in onset is highest (Figure 3). The “hit rate” for onset tercile values at high resolution given a low-resolution tercile value is very variable but generally only  $\sim 60\%$  for the early onset tercile and  $\sim 50\%$  for the late onset tercile.

It is higher in MAM than in OND, in which there are large parts of Kenya with very low “hit rates” for the late onsets (Figure 6k,m,n,p).

In contrast, for the AG1 onset metric the correlation between the two scales of analysis is generally only moderate in MAM ( $r < 0.6$  over much of the domain; Figure 6a) and low in OND ( $< 0.4$  over much of the domain; Figure 6b). Lower correlations are observed over parts of northwestern, central and eastern Kenya in OND as compared to MAM. The low correlation in AG1 can likely be attributed to the effect of spatial averaging on absolute rainfall values and hence the timing of exceedance of threshold values (Figure S10). The hit rate for the “perfect” forecast is much less in both seasons and especially so in OND with much of Kenya having less than 40% hit rate for late and early onset tercile categories (Figure 6f,h).

We conducted further spatial sensitivity analysis with MSWEP and CHIRPS (regridded) at  $0.1^\circ$  and  $1^\circ$  as detailed in sect. S2. Although MSWEP correlation is higher over the domain and thus contrasts with CHIRPS, especially in OND (Figures S11 and S12), the hit rate is  $< 50\%$  for much of Kenya, especially for AG1.

Overall, AA onsets are relatively insensitive to the scale of analysis, likely because the spatial autocorrelation in relative rainfall anomalies is quite high. As such AA represents a more robust onset metric than the

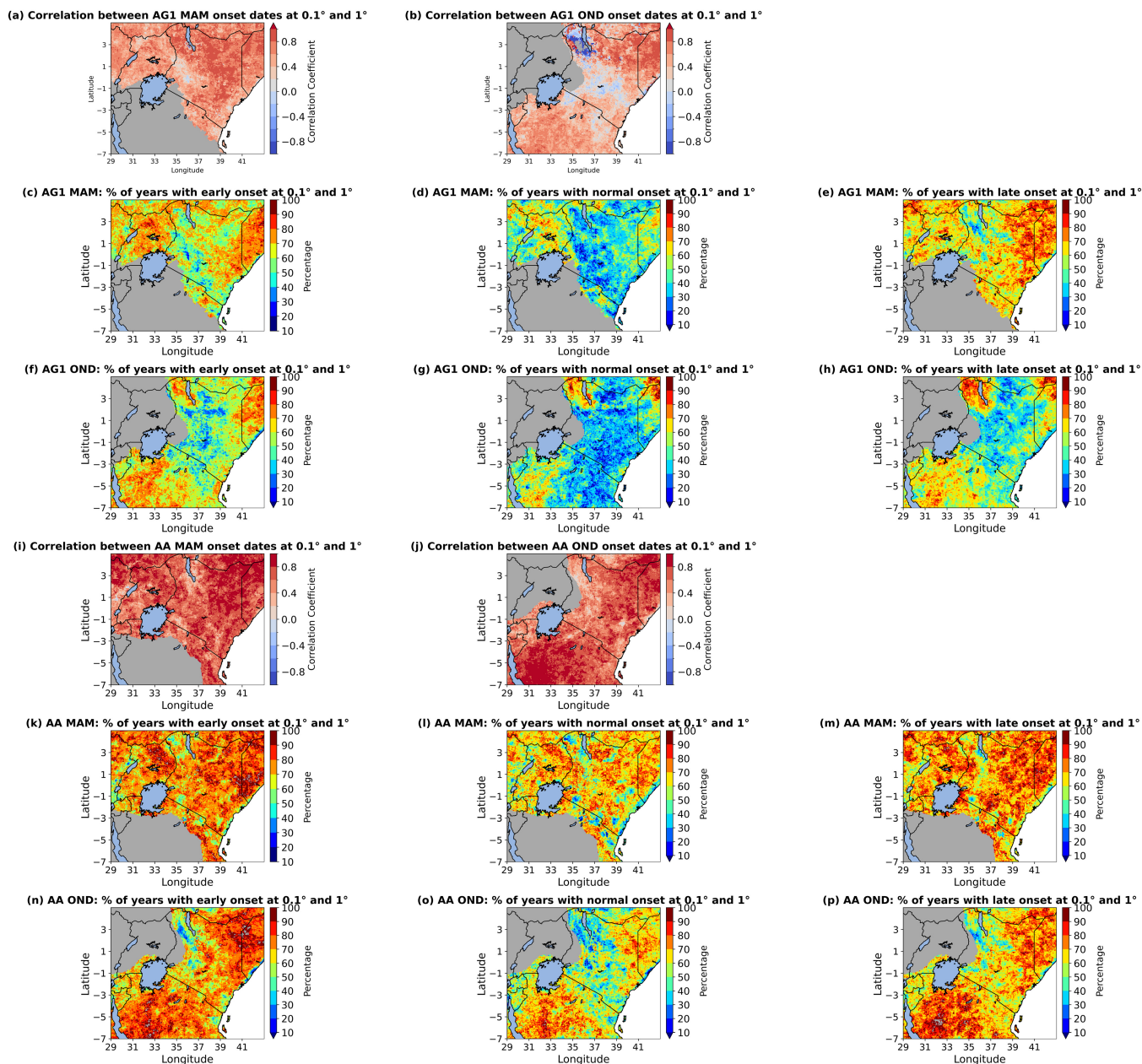


**FIGURE 6** Sensitivity of onset to spatial resolution of rainfall dataset. (a, b) Temporal correlation between onset dates at  $0.05^\circ$  and  $1^\circ$ ; for the AG1 metric during MAM and OND respectively. (i, j) Same as (a, b) but for the AA metric. (c–e) Percentage of years with the onset date in the same tercile category (early, normal, late, respectively) at  $0.05^\circ$  and  $1^\circ$  for MAM using AG1 metric. (f–h) Same as (c–e) but for OND. (k–m) Same as (c–e) but for the AA metric. (n–p) Same as (f–h) but for AA metric.

agronomic AG1. AG1 is not a robust onset indicator for onsets derived at a coarse scale e.g., from forecast models, for application at the local scale. Notwithstanding the potential for statistical artefacts in the gridded rainfall data, these results suggest that strong caution must be applied to the interpretation and use of coarse-scale climate information. We further infer that rainfall in OND is rather more spatially heterogeneous than in MAM.

Further, Figure 7 shows the sensitivity of onset variability to different rainfall datasets. Generally, in MAM, (Figure 7a–c) sensitivity to the dataset is variable but most areas show moderate to strong correlations. In OND (Figure 7d–f) however, correlation is notably lower for the agronomic AG1 and AG2 definitions, presumably reflecting the sensitivity of absolute rainfall thresholds to the more heterogeneous rainfall on OND (similar to the spatial scale analysis in Figure 6). The implication is that

## Correlation between CHIRPS 0.1° and MSWEP 0.1° onset dates

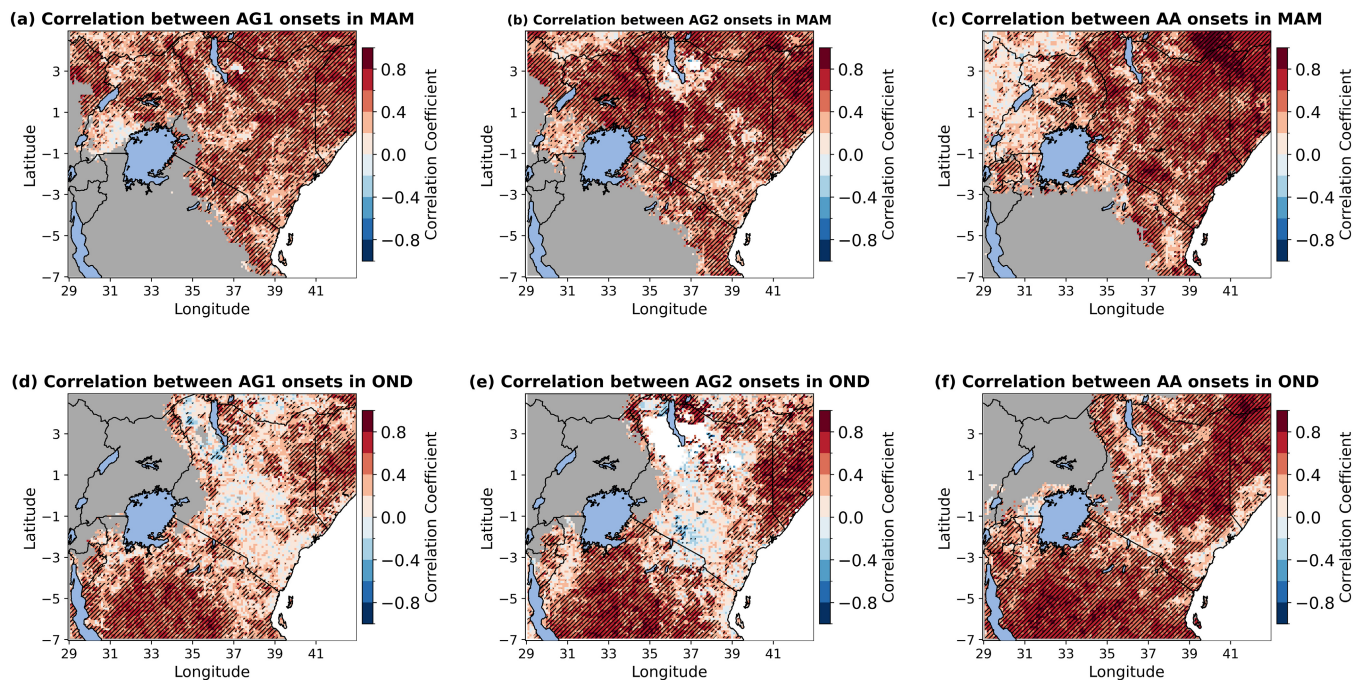


**FIGURE 7** Sensitivity of onset variability to different rainfall dataset. Temporal correlation between onset dates for CHIRPS 0.1° and MSWEP 0.1° for the three onset definition definitions; (a–c) MAM season and (d–f) OND season. Hatching represents correlations that are statistically significant at the 95% significance level.

agronomic definitions should be applied cautiously since they are highly sensitive to the data structure.

### 3.2 | Drivers of onset variability

Here we address research question 3 and explore the drivers of variability in onset across interannual (section 3.2.1) to subseasonal (section 3.2.2) timescales.

#### 3.2.1 | Large-scale drivers of onset variability at interannual timescales

That the spatial structures of onset variability (Figure 3d–fj–l) differ from those of seasonal total rainfall (Figure 1c,d) could imply that they are influenced by different drivers and/or respond differently to dominant driver systems. We explore these prioritizing results based on the AA definition since it incurs fewer instances when onset dates are not attained.

The OND leading EOF (Figure 8b; 22% of total variance) shows negative loadings over much of the domain and positive loading over a few areas along the western edge (Rift Valley) of the domain. This could be associated with the complexity of defining seasonality over the

region and the high interannual variability in seasonality. The associated PC1 time series has significant correlation with SSTs over the Indian and Pacific Oceans (Figure 8d) consistent with the well-established role of the IOD (Black, 2005; Hirons & Turner, 2018; Nicholson, 2017) and ENSO (Indeje et al., 2000; Mutai et al., 2012; Ogallo, 1988) in strongly driving OND rainfall. The reverse correlation of the IOD SST index and grid cell onset confirms this pattern of influence for all three onset definitions (Figure 8e–g), such that positive (negative) IOD events drive earlier (later) onset over much of the domain, consistent with Gudoshava et al. (2022a, 2022b), but later (earlier) onset along the western edge of the domain.

The difference that is noted along the Rift Valley with onset EOF and influence of the IOD on onset is not seen in seasonal rainfall. Seasonal rainfall shows positive correlation with IOD over much of the region with weaker correlation along the Rift Valley and Uganda (Figure S13). Further, the leading EOF of OND rainfall total reflects the IOD influence and loads uniformly over the region (Figure S14). Correlation of onset and total rainfall during the climatological season (Figure 9d–f) also shows the differing pattern along the western edge of the domain while we see the expected negative correlation over the rest of the domain, consistent with

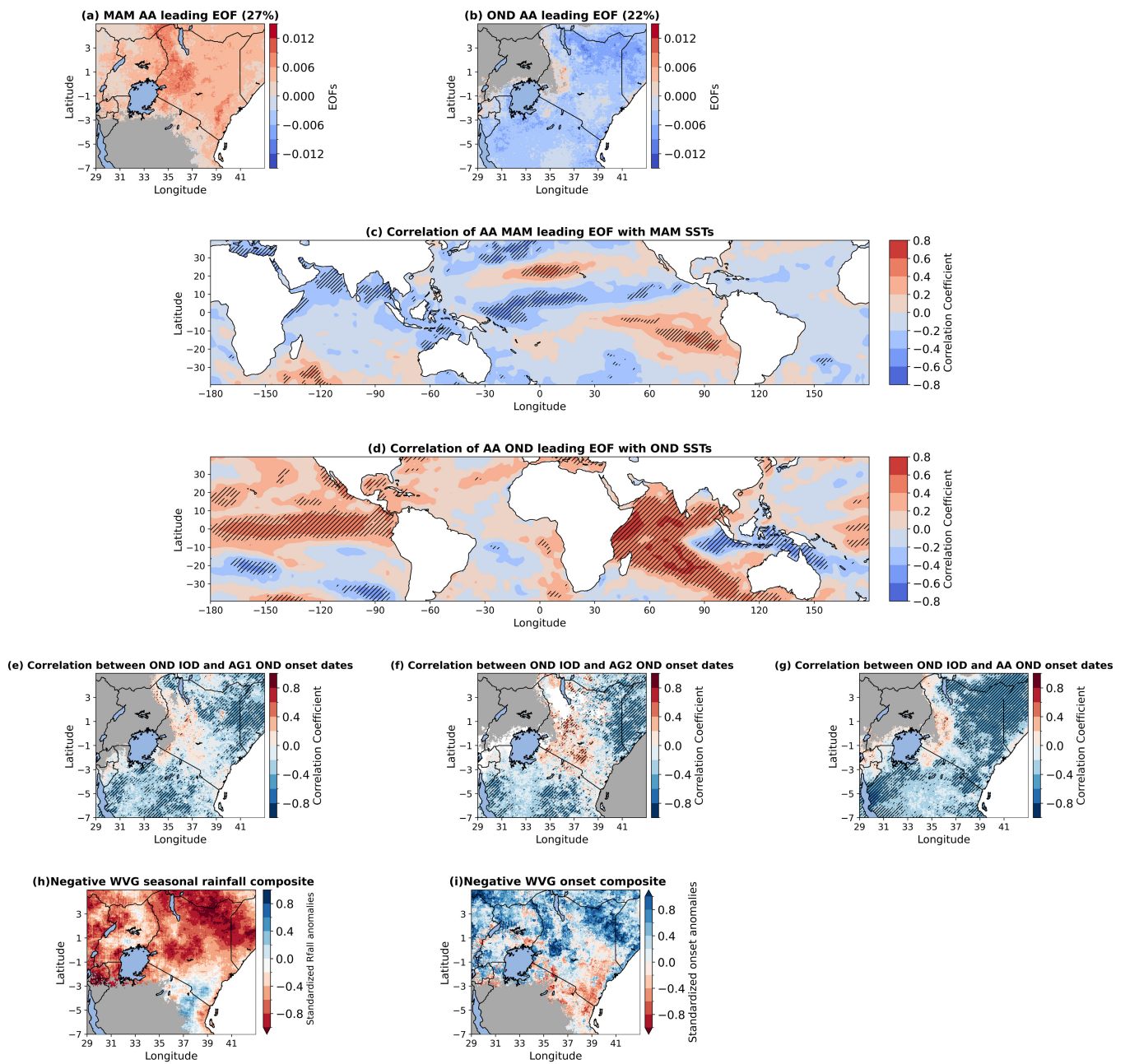


**FIGURE 8** Leading EOF loadings of AA onset dates for; (a) MAM and (b) OND. Correlation between; (c) MAM leading EOF PCs and MAM SSTs (b) OND leading EOF PCs and OND SSTs; (e–g) OND IOD index with OND onset dates for, AG1, AG2 and AA, respectively. Composites of; (h, i) negative WVG rainfall and MAM AA onset dates respectively. Hatching represents correlations that are statistically significant at the 95% significance level.

Camberlin et al. (2019) and MacLeod (2018). The differing pattern along the edge reflects the effects of complex seasonality and the high interannual variability in seasonality on onset definition and hence linkage to interannual drivers.

In the MAM season, the leading EOF (Figure 8a, 27% of total variance) shows the highest loadings over the Rift Valley, Western, Central and Coastal Kenya. Correlation of the leading EOF PCs with MAM SSTs indicates low

correlation over most tropical oceans (Figure 8c), consistent with documented relatively low sensitivity of MAM total rainfall variability to tropical modes of SSTs (Mutai & Ward, 2000; Ogallo, 1988). However, significant correlations over the Arabian Sea and Southern Indian Ocean are consistent with the findings of Wainwright et al. (2019) suggesting that warmer SSTs to the South of Madagascar (over Arabian Sea) drive a delayed (faster) northward progression of the rain belt resulting in late

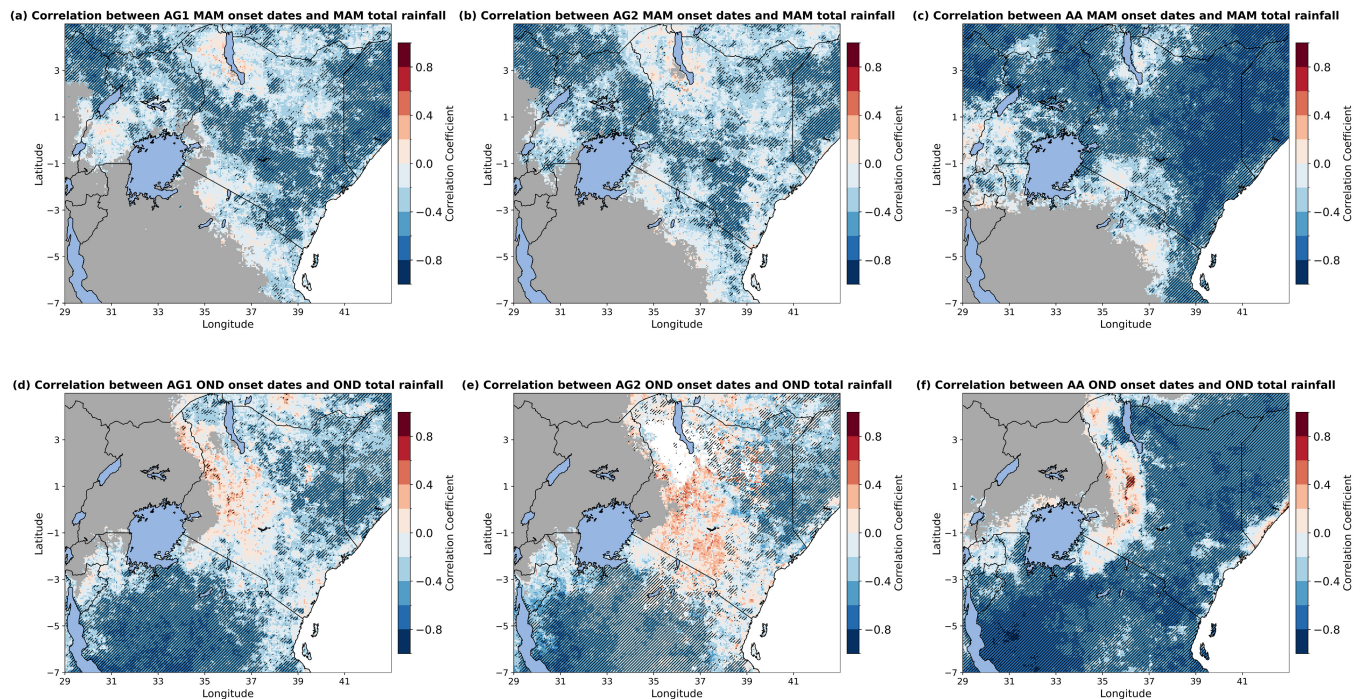


**FIGURE 9** Temporal correlation between total seasonal rainfall and onset dates; (a–c) MAM season with AG1, AG2 and AA definitions, respectively, (d–f) Same as (a–c) but for OND. Hatching represents correlations that are statistically significant at the 95% significance level.

(early) onset. We also see significant negative (positive) correlations between MAM onset and SSTs in the central (eastern) Pacific. This pattern is very similar to that identified by Maybee et al. (2022) in driving both MAM rainfall over the Greater Horn of Africa (GHA) and the activity of the MJO, whose activity in phases 1–3 they report drives variability in GHA rainfall. So while this provides an indication of commonality between drivers of interannual variability in both seasonal rainfall and onset, the role of subseasonal MJO activity is highlighted (and by Vellinga & Milton, 2018) and we explore this specifically in relation to onset in section 3.2.2. Further, this Pacific SST pattern in Figure 8c is also reminiscent of the WVG pattern which drives an asymmetric response to EA rainfall, such that it is the negative WVG phase that drives a stronger, dry MAM, signal over EA (Funk et al., 2023). Composites during major negative WVG MAM seasons (in which WVG index  $< -1$ ) show negative total rainfall anomalies and late onsets (positive anomalies) over much of Kenya and Uganda (Figure 8h,i), although the onset signal is weaker and less consistent spatially. As such we find a rather weak association of onset with the Western V mode.

In line with the leading EOF pattern, MAM onset dates (notably for the AA metric; Figure 9c) have a strong significant negative correlation with MAM total rainfall

over much of the domain (Figure 9a–c). Kijazi and Reason (2012) documented that anomalously wet MAM seasons over the Northeastern Highlands of Tanzania are associated with earlier onsets. MacLeod (2018) also showed this kind of correlation in the region.

### 3.2.2 | From interannual to intraseasonal influences: Identifying unusually early or late onset “deviant” years

The preceding results suggest strong controls on the onset known modes of interannual variability. However, at most (during OND in the Eastern part of the domain) only  $\sim 50\%$  of the variance in onset dates is explained by seasonal rainfall. As such, there remains a dominant proportion of onset variance which is not clearly associated with interannual drivers. In this section, for both OND and MAM, we examine 2 years in which unusually early or late onset most strongly deviates from that expected from the interannual signal (see section 2 and Figure S15). We assess the role of the MJO in each case. Previous analysis has established that MJO in phases 1–4 (5–8) favours enhanced (suppressed) rainfall in the region (Camberlin et al., 2019; Kilavi et al., 2018; MacLeod et al., 2021; Maybee et al., 2022; Zaitchik, 2017)

## MAM: Unusually early years

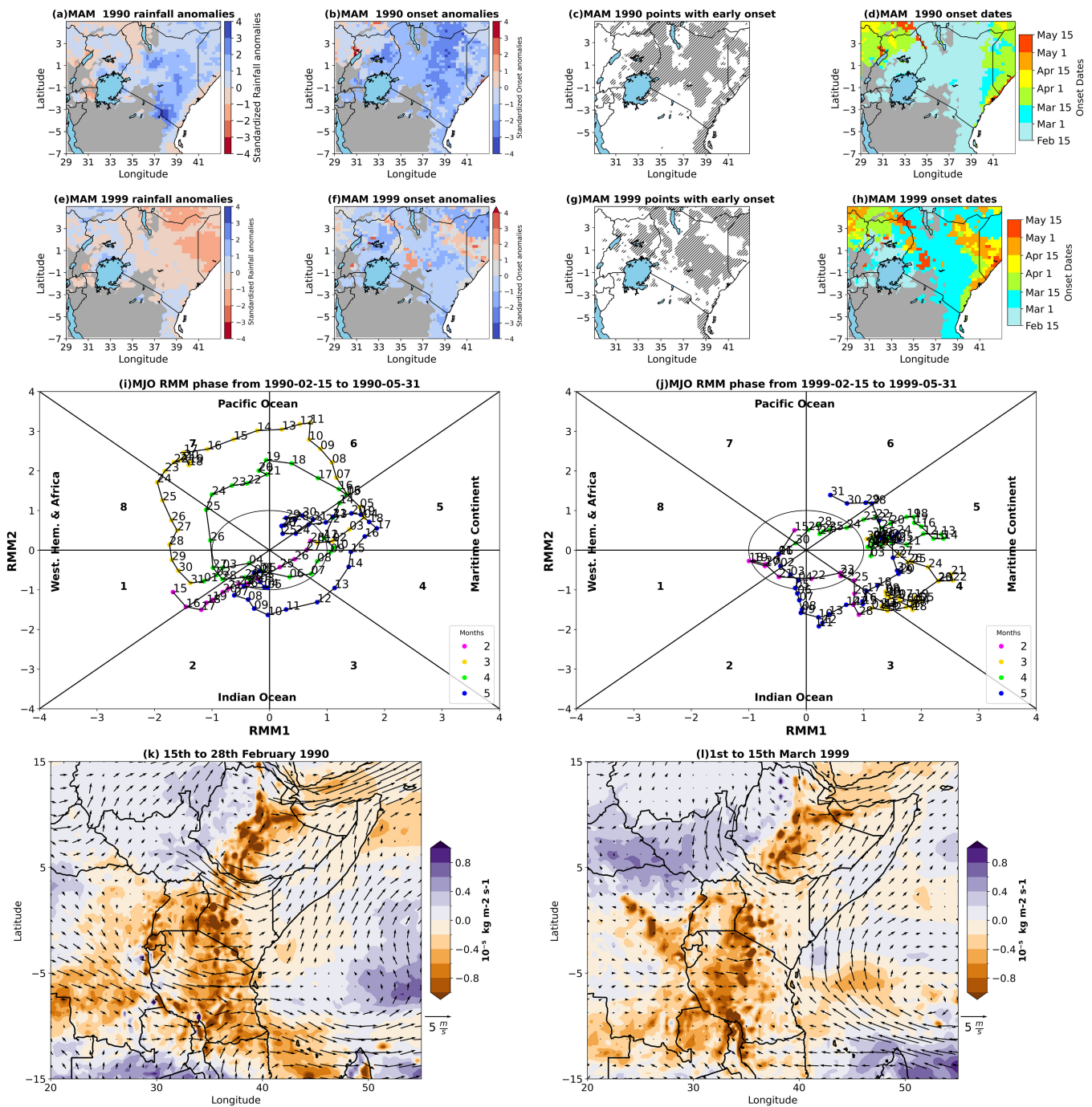


**FIGURE 10** Onset conditions at subseasonal timescales during the two most “deviant” MAM early onset seasons of MAM 1990 (a–d), (i), (k) and MAM 1999 (e–h), (j), (l), respectively. (a, e) Standardized rainfall anomalies, (b, f) standardized onset anomalies, (c, g) locations of deviant grid cells and (d, h) onset dates. These are only shown where the correlation between seasonal rainfall and onset date is statistically significant (based on Figure 9). (i, j) The evolution of the MJO phase and magnitude using the RMM diagram (see section 2). (k, l) Circulation diagnostics of anomalous vertically integrated moisture divergence ( $\text{kg}\cdot\text{m}^{-2}\cdot\text{s}^{-1}$ ) and 850 hPa winds (vector magnitude is shown on plot), during the dominant onset periods of (k) 15th–28th February 1990 (consistent with (c, d)), and (l) 1st–15th March 1999 (consistent with (g, h)).

(Readers are reminded of the influence of the MJO phase on EA rainfall in Figures S6 and S7). MJO phases 3 and 4 (and to some extent phase 2) have been associated with

the likely occurrence of westerly flow anomalies resulting in enhanced rainfall over EA (Berhane & Zaitchik, 2014; Finney et al., 2020; Pohl & Camberlin, 2006).

MAM: Unusually late years

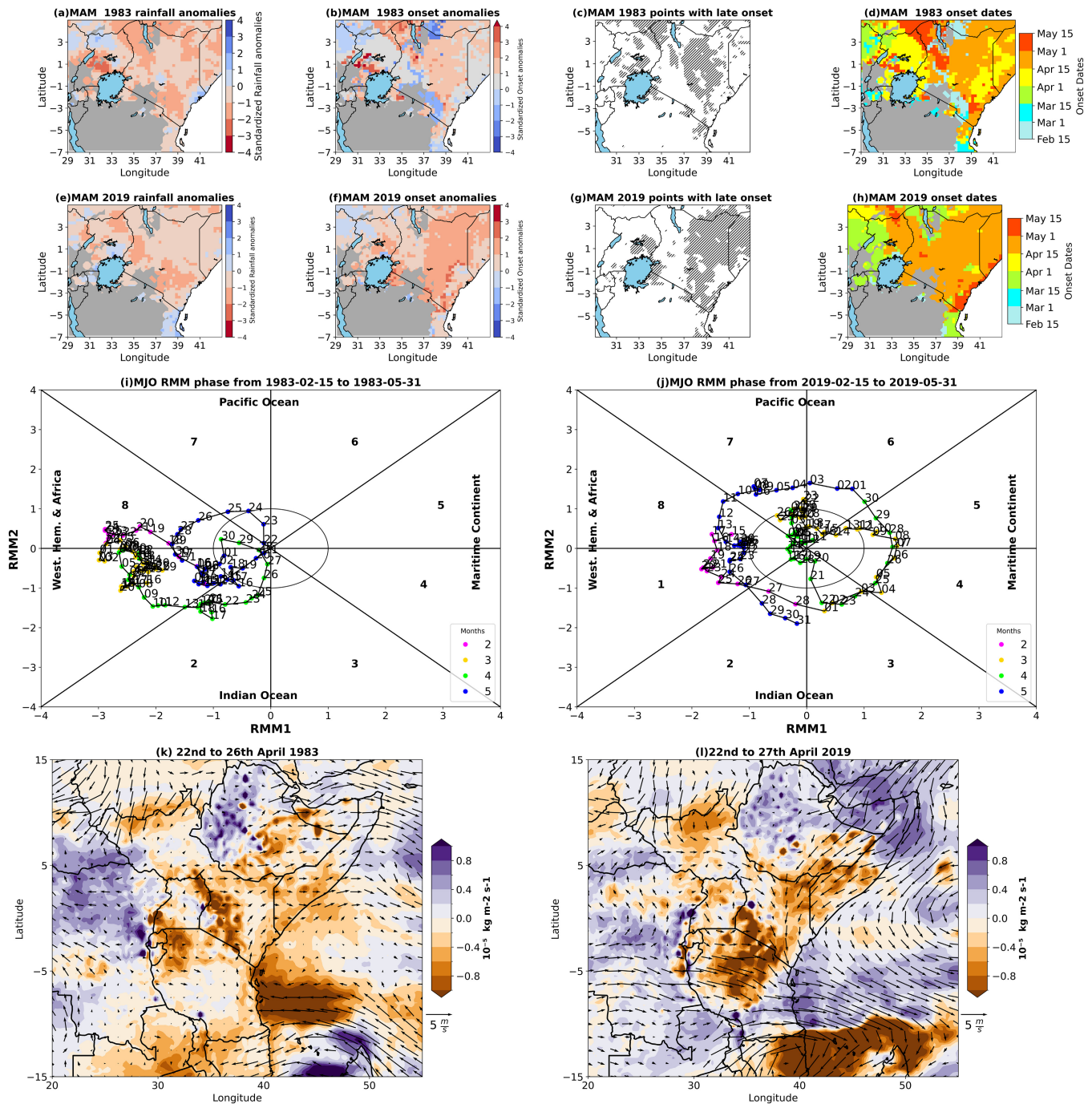


**FIGURE 11** Onset conditions at subseasonal timescales during two “deviant” MAM late onset seasons of MAM 1983 (a–d), (i), (k) and MAM 2019 (e–h), (j), (l), respectively. (a, e) Standardized rainfall anomalies, (b, f) standardized onset anomalies, (c, g) locations of deviant grid cells and (d, h) onset dates. These are only shown where the correlation between seasonal rainfall and onset date is statistically significant (based on Figure 9). (i, j) The evolution of the MJO phase and magnitude using the RMM diagram (see section 2). (k, l) Circulation diagnostics of anomalous vertically integrated moisture divergence ( $\text{kg}\cdot\text{m}^{-2}\cdot\text{s}^{-1}$ ) and 850 hPa winds (vector magnitude is shown on plot), during the dominant onset periods of (k) 22nd–26th February 1983 (consistent with (c, d)), and (l) 22nd–27th April 2019 (consistent with (g, h)).

For unusually early onset in MAM, 1990 and 1999 are the 1st and 3rd most extensive “deviant” years (Figure S16). In both cases, onset was unusually early

over much of Kenya, southern Somalia, and eastern Uganda (Figure 10b,f) although the seasonal rainfall conditions are contrasting. (Note that the 2nd largest year,

2010, is presented in Figure S15 as the seasonal conditions are similar to those of 1990). In MAM 1990 onset was exceptionally early (Figure 10b,c), occurring in late February (Figure 10d). This early onset coincided with MJO in phase 2 with high amplitude (Figure 10i) which favours enhanced rainfall over EA (Figure S7), and widespread anomalous moisture convergence in westerly flow anomalies (Figure 10k), consistent with the dynamical analysis of Finney et al. (2020). During the remainder of the season, the MJO remained active in all phases, including many days in phases 1–4 both of which are consistent with anomalously wet seasonal conditions (Maybee et al., 2022; Vellinga & Milton, 2018). As such, in MAM 1990 MJO activity is consistent with both the triggering of a very early onset and high rainfall conditions throughout the season.

MAM 1999 differed in that the season was drier than normal (Figure 10e), yet onset was unusually early (Figure 10f,g) occurring mostly in early March (Figure 10h). Onset coincided with an active MJO in phase 3–4 (Figure 10j) which favours enhanced rainfall over EA (Figure S7) and anomalous westerly moisture flux and convergence over much of the region (Figure 10l) this is consistent with earlier studies that have linked enhanced rainfall over the region to westerly flow anomalies (Camberlin & Wairoto, 1997; Dyer & Washington, 2021). The MJO was strongly active in phases 5 and 6 for much of the rest of the season which favours suppressed rainfall over EA (Figure S7). As such, the MJO activity is consistent with both the early onset and subsequent suppressed rainy season.

For deviant late onset MAM seasons, we consider 1983 and 2019 which are the 2nd and 3rd most deviant seasons (Figure S15). (Note that 1st most deviant season, MAM 2003 (see Figure S16) has a spatially incoherent distribution of deviant grid cells and onset dates rendering identification of coherent drivers problematic). In MAM 1983, onset was unusually late over much of Eastern Kenya (Figure 11b,c) and seasonal rainfall was below average over the region (Figure 11a). Although active, the MJO was in phases 8 and 1 for much of March and early April which is consistent with drier conditions over the region (Figure S7) (MacLeod et al., 2021; Maybee et al., 2022). The late onset in late April over Eastern Kenya coincided with active MJO in phase 2 (Figure 11i) and moisture convergence in easterly flow (Figure 11k); this is consistent with the analysis of Pohl and Camberlin (2006). For much of the season, the MJO was in phases 7 and 8 for many days, which is associated with suppressed rainfall. Thus, MJO activity is consistent with the late triggering of onset and suppressed rainfall during the season.

In MAM 2019, onset was unusually very late over Eastern Kenya, Southern Somalia and parts of the Lake Victoria basin (Figure 11f,g), occurring in mid-April (Figure 11h). Seasonal rainfall was low but not strongly so (Figure 11e). MJO activity was suppressed during much of late March to mid-April consistent with dry conditions. The onset in late April coincided with active MJO in phase 3 (Figure 11j) and moisture convergence (Figure 11l). During MAM 2019 under the ForPac project ([www.forpac.org](http://www.forpac.org)) the UK Met Office piloted provision to the Kenya Meteorological Department (KMD) of subseasonal forecasts of weekly rainfall out to 4 weeks lead time from the GloSEA5 model. On the basis of these forecasts, KMD issued a forecast of a 3–4 week delay in expected onset (White et al., 2022). This updated their earlier long lead seasonal forecast and was useful for adjusting farming activities such as planting. Note that from late February to early March, the MJO was active in phases 2 and 3 but it did not trigger onset as the moisture convergence belt was further to the south, likely associated with the strong influence of tropical cyclone Idai which propagated from the over the Southwest Indian Ocean into continental Southern Africa (Figure S17).

For OND we consider the 1st and 2nd most deviant early onset seasons of 2011 and 2017. In OND 2011, onset was earlier than usual over parts of Eastern Kenya (Figure 12b,c), although total seasonal rainfall was below average (Figure 12a). The early onset occurred in mid-October (Figure 12d) and coincides with the MJO in phase 2 (Figure 12i), which favours enhanced rainfall over Kenya (Figure S8) (Camberlin et al., 2019) and moisture convergence (Figure 12k). For the rest of the season, the MJO is in phases 4 and 5 which suppresses rainfall over the eastern sector of the region (ibid) MJO activity is thus consistent with early onset and below-average rainfall over parts of Eastern Kenya. In OND 2017, earlier than usual onset occurred over eastern Kenya and parts of Tanzania (Figure 12f,g) despite below-average seasonal rainfall over these areas (Figure 12e). Over some of these areas the unusually early onset occurred at the beginning of October (Figure 12h) coinciding with MJO phases 2 and 3 (Figure 12j) which is consistent with enhanced rainfall and convergence in the westerly flow anomalies (Figure 12l). For much of the season, the MJO was active in phases 5 and 6 which are associated with suppressed rainfall over the region (Figure S8).

For OND deviant late onset seasons, we consider 1991 and 2006. In OND 1991, onset was later than usual in parts of Central Tanzania and Northeastern Kenya (Figure 13b,c) and total rainfall was generally below average over these areas (Figure 13i). For much of October, the MJO was inactive and in November the MJO was

OND: Unusually early years

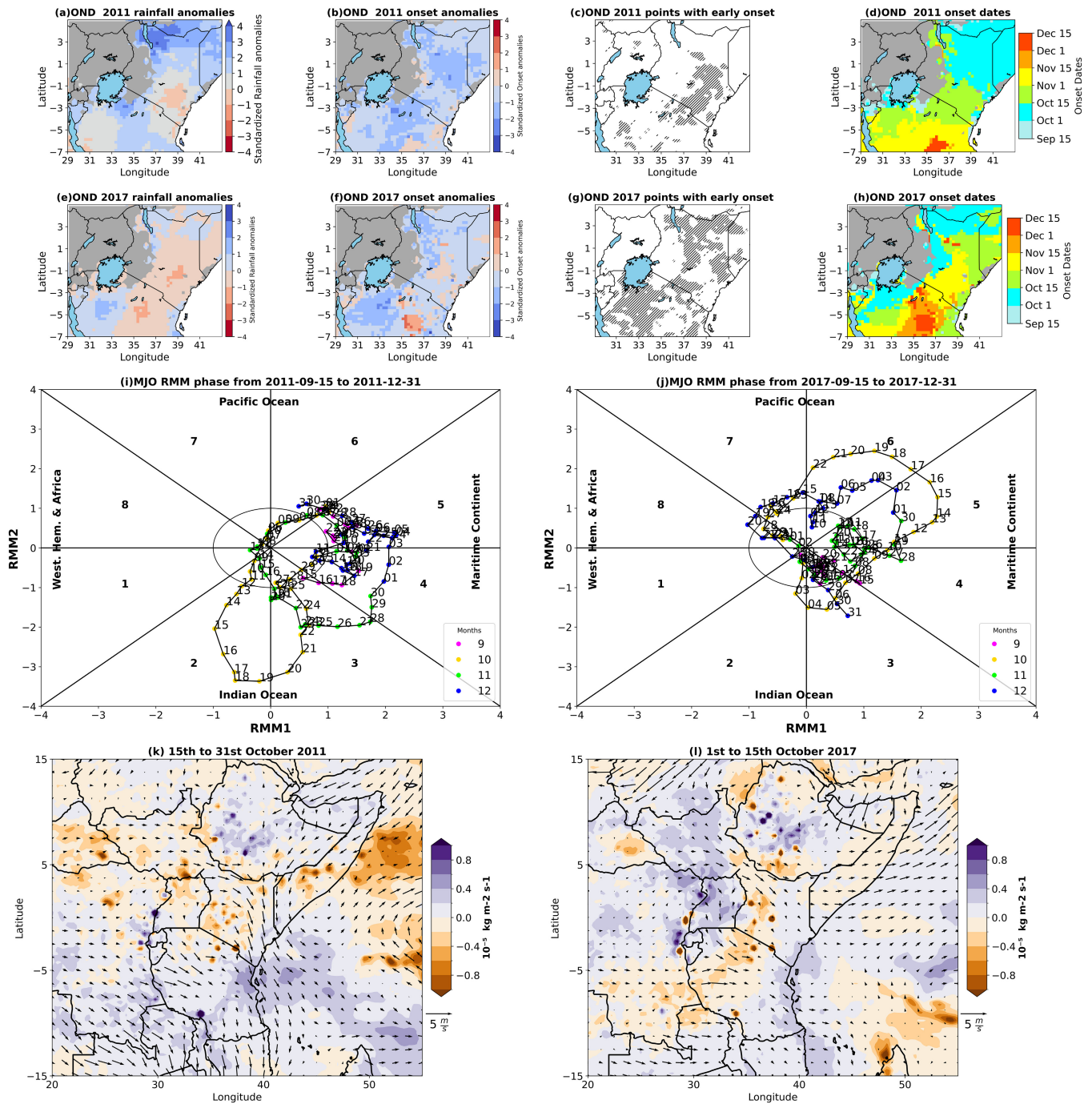


**FIGURE 12** Onset conditions at subseasonal timescales during the two most “deviant” OND early onset seasons of OND 2011 (a–d), (i), (k) and OND 2017 (e–h), (j), (l), respectively. (a, e) Standardized rainfall anomalies, (b, f) standardized onset anomalies, (c, g) locations of deviant grid cells and (d, h) onset dates. These are only shown where the correlation between seasonal rainfall and onset date is statistically significant (based on Figure 9). (i, j) The evolution of the MJO phase and magnitude using the RMM diagram (see section 2). (k, l) Circulation diagnostics of anomalous vertically integrated moisture divergence ( $\text{kg}\cdot\text{m}^{-2}\cdot\text{s}^{-1}$ ) and 850 hPa winds (vector magnitude is shown on plot), during the dominant onset periods of (k) 15th–31st October 2011 (consistent with (c, d)), and (l) 1st to 5th October 2017 (consistent with (g, h)).

mostly active in Phase 8 which is associated with suppressed rainfall over much of the region except the Coast (Figure S8). Onset occurred from early to mid-December

(Figure 13d) coinciding with MJO in phase 1 (Figure 13i) and strong convergence over Tanzania (Figure 13k) this is consistent with slightly enhanced rainfall over parts of

## OND: Unusually late years

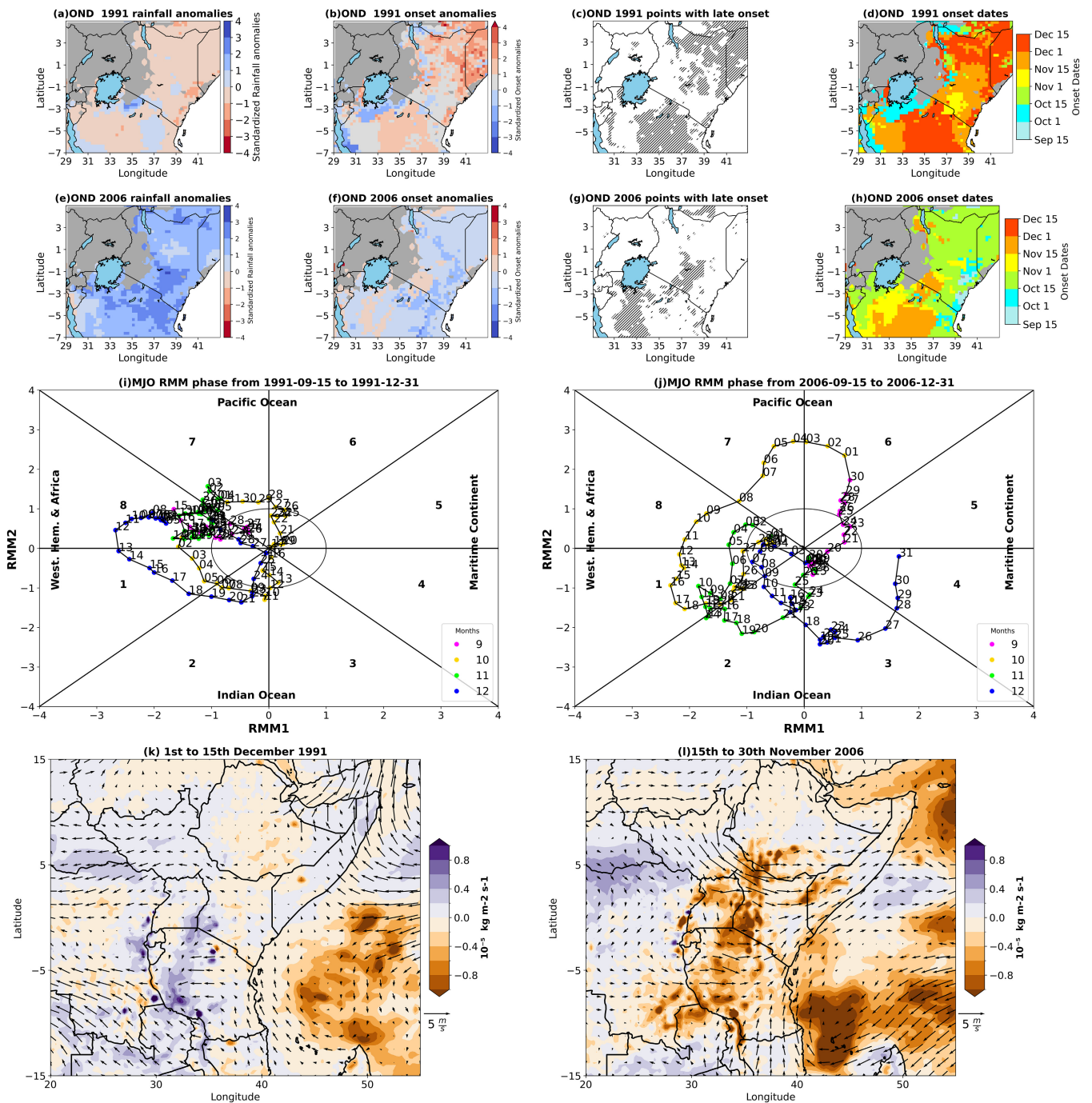


**FIGURE 13** Onset conditions at subseasonal timescales during the two most "deviant" OND late onset seasons of OND 1991 (a–d), (i), (k) and OND 2006 (e–h), (j), (l), respectively. (a, e) Standardized rainfall anomalies, (b, f) standardized onset anomalies, (c, g) locations of deviant grid cells and (d, h) onset dates. These are only shown where the correlation between seasonal rainfall and onset date is statistically significant (based on Figure 9). (i, j) The evolution of the MJO phase and magnitude using the RMM diagram (see section 2). (k, l) Circulation diagnostics of anomalous vertically integrated moisture divergence ( $\text{kg m}^{-2} \text{s}^{-1}$ ) and 850 hPa winds (vector magnitude is shown on plot), during the dominant onset periods of (k) 1st to 15th December 1991 (consistent with (c, d)), and (l) 15th–30th November 2006 (consistent with (g, h)).

Tanzania (Figure S8). MJO activity triggered the late onset and suppressed rainfall during the season. In contrast, OND 2006 had an above-average rainfall

(Figure 13e) and earlier onset over much of the region (Figure 13f) except Southern Kenya and Central Tanzania (Figure 13g). The late onset occurred in Mid-

November and coincided with MJO in Phase 2 which is associated with enhanced rainfall over these areas (Figure S8) and convergence (Figure 131). For much of the season, the MJO was in phases 1, 2 and 3 which are associated with enhanced rainfall over the region hence the wetter-than-average season.

In summary, our analysis indicates that onset during the deviant seasons is often triggered by MJO being in phases 2 and 3, consistent with the established role of MJO in the region. This provides a clear indication of the potential for improved forecasting of onset at subseasonal lead times, as demonstrated in the pilot case study in MAM 2019 over Kenya. Further, our results suggest the MJO also influences the outcome of the entire season, with seasons that are drier than usual, having MJO in unfavourable phases for much of the season (MAM 2019, OND 2017). While wetter than usual seasons have the MJO largely in favourable phases (MAM 1990). This concurs with studies that associate MJO activity with seasonal outcomes (Maybee et al., 2022; Vellinga & Milton, 2018).

## 4 | CONCLUSION AND RECOMMENDATIONS

A sound understanding of onset variability and the associated drivers are essential for forecasting and subsequent application in risk management. For the East Africa region, this paper seeks to provide a comprehensive and systematic assessment of various onset definition definitions and onset variability and drivers, across time scales.

Climatological onset dates from the three candidate onset definitions evaluated are similar to those derived in earlier studies for both wet seasons (Camberlin & Okoola, 2003; Dunning et al., 2016; Gudoshava et al., 2022a, 2022b; MacLeod, 2018). However, the heterogeneity of variability in onset is only very broadly consistent across definitions and has large differences in local detail. Crucially, onset is most variable over many of the high-production agricultural areas, and this potentially has implications for agricultural and risk management decision-making. The complex seasonality over the region and high interannual variability in seasonality over western sector does affect the definition of rainy season onset and thus there is no broad rule that is applicable over the region. This challenge is evident in the broad season categorisations and sometimes lack of specificity in operational onset forecast products. Livelihood calendars in some of the complex regions seem to give a better understanding of seasonality and influence on agricultural activities.

Notably, the temporal correlation among definitions is low over the region, especially in the OND season such that the choice of metric is clearly a key consideration in the provision of onset information. Further, due to marked climatic gradients across EA agronomic definitions utilized in current operational forecasts provided by meteorological agencies in the region are not well suited for region-wide application. Thus, operational onset definitions should be fine-tuned to specific livelihoods and agricultural needs through a process of co-production with relevant stakeholders. Although the accumulated anomaly AA metric which provides onset timing relative to local climate is more robust, there is a need to evaluate the utility of this metric to support decision-making in agricultural practices or other applications.

Agronomic definitions are also particularly sensitive to the spatial scale of analysis and to the choice of rainfall dataset. This is due to the sensitivity of the absolute rainfall threshold values to rainfall variability and uncertainties. Information provided at coarse scales is typically not strongly applicable to decision-making at local level. Even for the most robust metric (AA), a perfect forecast would have limited “skill” at the local level, with a hit rate of below 60% over large areas, for late tercile onset events. Therefore, onset forecasts, especially using agronomic definitions, should be issued, and interpreted cautiously given this scale sensitivity.

Onset emerges from a complex interaction of inter-annual and subseasonal drivers. The interannual variability in onset is influenced by the same large-scale modes that influence total seasonal rainfall. Onset variability in OND is driven by the IOD and ENSO with IOD likely the most dominant. MAM onset has weak association with the Pacific “Western V Gradient” SST pattern. Onset is found to have a high correlation with total rainfall over much of the region for both seasons. Indeed, although correlation between onset and total rainfall during the climatological season is high in many areas this explains at most about 50% of onset variance. As such the shorter-term subseasonal drivers of onset must be considered. For the seasons in which onset deviates most strongly from the influence of seasonal scale controls we identify subseasonal influences on onset, notably from the MJO. In many of these seasons, the MJO also likely influences the characteristics of the rest of the season, especially so for the MAM season.

We make the following recommendations consistent with our results. The region has a complex seasonality that has implications on definition of onset and the use of updated livelihood calendars could inform definition of seasons and provision of forecast information that aligns with diverse livelihood activities. The choice of

onset metric in each season is important, and agronomic definitions should be applied cautiously as they are especially sensitive to spatial averaging and data uncertainties. This points to a stronger need for co-production of onset information, in which meteorological agencies work with stakeholders to define actionable onset definitions and to establish the appropriate use of coarse-scale onset monitoring and forecast information at the local level. This should be informed by a co-produced assessment of skill and salience of coarse-scale onset information to risk management decisions across spatial scales and across forecast lead times. An assessment of subseasonal onset forecast skill directly in relation to risk management decisions will be reported by the authors in a companion paper. Such systematic analysis of the credibility and salience of onset information and the further enhancement of co-production processes are therefore a key priority. This is especially so given the demand for climate information and indeed the ongoing development of agricultural decision support tools ingesting forecast information targeted at local-level stakeholders (e.g., Black et al., 2023).

Advances in global forecast models reveal EA to be a “sweet spot” of predictability, at subseasonal scales across all seasons (de Andrade et al., 2021; MacLeod et al., 2021). This presents a basis for provision of onset forecasts across “seamless” seasonal to subseasonal lead timescales. Onset forecasts at the seasonal lead times could provide a “heads-up” of what is expected, especially in years when the main interannual drivers are active. Subsequent updates of onset timing from subseasonal forecasts could then be issued, perhaps on a weekly basis (as with the products during the S2S real time pilot project), to inform the implementation of onset-related activities. Further, recent experience in the provision of subseasonal rainfall forecasts through the “Forecasts for Preparedness Action” (ForPac, [www.forpac.org](http://www.forpac.org)) project suggests that a narrative explanation of the underlying drivers, for example, the state of the MJO and associated teleconnections, can usefully augment subseasonal forecasts and add confidence in stakeholder interpretation (White et al., 2022). Our results here reinforce the call for enhanced forecasting capability in EA Meteorological services, continued access to subseasonal forecasting information from global modelling centres, and for enhanced and continued co-production between meteorological services and stakeholders to make most effective use of forecast skill in EA, in line with the growing body of evidence in the region (Gudoshava et al., 2022b; Hirons et al., 2021; Muita et al., 2021; Mwangi et al., 2022). Such activities can ensure advantage is taken from the opportunity afforded by relatively high climate predictability in EA across subseasonal to seasonal timescales.

## AUTHOR CONTRIBUTIONS

**Emmah Mwangi:** Writing – original draft; conceptualization; methodology; formal analysis. **Dave MacLeod:** Methodology; writing – review and editing; supervision. **Martin C. Todd:** Supervision; writing – review and editing; methodology. **Dominic Kniveton:** Supervision; writing – review and editing.

## ACKNOWLEDGEMENTS

This research was supported by the Science for Humanitarian Emergencies and Resilience (SHEAR) consortium project “Towards Forecast-based Preparedness Action” (ForPac, [www.forpac.org](http://www.forpac.org); Grant Nos. NE/P000673/1, NE/P000568/1, NE/P000428/1 and NE/P000444/1). The SHEAR programme is funded by the UK Natural Environment Research Council, the Economic and Social Research Council and the UK Department for International Development. Emmah Mwangi is supported through the generous donation of the Sussex University Scholarship programme.

## DATA AVAILABILITY STATEMENT

The datasets that support the findings of this study are openly available at the following links: (i) [https://data.chc.ucsb.edu/products/CHIRPS-2.0/global\\_daily/netcdf/p05/](https://data.chc.ucsb.edu/products/CHIRPS-2.0/global_daily/netcdf/p05/) and <https://www.gloh2o.org/mswep/> for CHIRPS and MSWEP rainfall datasets, (ii) <https://psl.noaa.gov/data/gridded/data.noaa.oisst.v2.html> for sea surface temperatures and (iii) <https://cds.climate.copernicus.eu/cdsapp#!/search?type=dataset> for 850 hPa zonal winds and vertically integrated moisture divergence.

## ORCID

Emmah Mwangi  <https://orcid.org/0000-0003-3838-0849>

## REFERENCES

- Acharya, N. & Bennett, E. (2021) Characteristic of the regional rainy season onset over Vietnam: tailoring to agricultural application. *Atmosphere*, 12(2), 198. Available from: <https://doi.org/10.3390/atmos12020198>
- Beck, H.E., Wood, E.F., Pan, M., Fisher, C.K., Miralles, D.G., van Dijk, A.I.J.M. et al. (2019) MSWEP V2 global 3-hourly 0.1° precipitation: methodology and quantitative assessment. *Bulletin of the American Meteorological Society*, 100(3), 473–500. Available from: <https://doi.org/10.1175/BAMS-D-17-0138.1>
- Berhane, F. & Zaitchik, B. (2014) Modulation of daily precipitation over East Africa by the Madden–Julian Oscillation. *Journal of Climate*, 27(15), 6016–6034. Available from: <https://doi.org/10.1175/JCLI-D-13-00693.1>
- Black, E. (2005) The relationship between Indian Ocean sea-surface temperature and East African rainfall. *Philosophical Transactions of the Royal Society A: Mathematical, Physical and Engineering Sciences*, 363(1826), 43–47. Available from: <https://doi.org/10.1098/rsta.2004.1474>
- Black, E., Asfaw, D.T., Sananka, A., Aston, S., Boulton, V.L. & Maidment, R.I. (2023) Application of TAMSAT-ALERT soil

- moisture forecasts for planting date decision support in Africa. *Frontiers in Climate*, 4, 993511. Available from: <https://doi.org/10.3389/fclim.2022.993511>
- Camberlin, P. & Okoola, R.E. (2003) The onset and cessation of the “long rains” in eastern Africa and their interannual variability. *Theoretical and Applied Climatology*, 75(1), 43–54. Available from: <https://doi.org/10.1007/s00704-002-0721-5>
- Camberlin, P. & Wairoto, J.G. (1997) Intraseasonal wind anomalies related to wet and dry spells during the “long” and “short” rainy seasons in Kenya. *Theoretical and Applied Climatology*, 58(1–2), 57–69. Available from: <https://doi.org/10.1007/BF00867432>
- Camberlin, P., Gitau, W., Kiladis, G., Bosire, E. & Pohl, B. (2019) Intraseasonal to interannual modulation of diurnal precipitation distribution over eastern Africa. *Journal of Geophysical Research: Atmospheres*, 124(22), 11863–11886. Available from: <https://doi.org/10.1029/2019JD031167>
- de Andrade, F.M., Coelho, C.A.S. & Cavalcanti, I.F.A. (2019) Global precipitation hindcast quality assessment of the subseasonal to seasonal (S2S) prediction project models. *Climate Dynamics*, 52(9–10), 5451–5475. Available from: <https://doi.org/10.1007/s00382-018-4457-z>
- de Andrade, F.M., Young, M.P., MacLeod, D., Hirons, L.C., Woolnough, S.J. & Black, E. (2021) Subseasonal precipitation prediction for Africa: forecast evaluation and sources of predictability. *Weather and Forecasting*, 36(1), 265–284. Available from: <https://doi.org/10.1175/WAF-D-20-0054.1>
- Dunning, C.M., Black, E.C.L. & Allan, R.P. (2016) The onset and cessation of seasonal rainfall over Africa. *Journal of Geophysical Research: Atmospheres*, 121(19), 11405–11424. Available from: <https://doi.org/10.1002/2016JD025428>
- Dyer, E. & Washington, R. (2021) Kenyan long rains: a subseasonal approach to process-based diagnostics. *Journal of Climate*, 34(9), 3311–3326. Available from: <https://doi.org/10.1175/JCLI-D-19-0914.1>
- Famine Early Warning Systems Network (FEWSNET). (2011) Kenya—livelihood description. Available from: <https://fewsn.net/east-africa/kenya/livelihood-description/march-2011>
- Feed the Future. (2019) Kenya’s March-to-May season: an examination of April 2019 predictions, May 2019 outcomes, and the implications of a poor start to the season|Agrilinks. Available from: <http://agrilinks.org/post/kenyas-march-may-season-examination-april-2019-predictions-may-2019-outcomes-and-implications>
- Ferijal, T., Batelaan, O., Shanafield, M. & Alfahmi, F. (2022) Determination of rainy season onset and cessation based on a flexible driest period. *Theoretical and Applied Climatology*, 148(1–2), 91–104. Available from: <https://doi.org/10.1007/s00704-021-03917-1>
- Finney, D.L., Marsham, J.H., Walker, D.P., Birch, C.E., Woodhams, B.J., Jackson, L.S. et al. (2020) The effect of westerlies on East African rainfall and the associated role of tropical cyclones and the Madden–Julian Oscillation. *Quarterly Journal of the Royal Meteorological Society*, 146(727), 647–664. Available from: <https://doi.org/10.1002/qj.3698>
- Fitzpatrick, R.G.J., Bain, C.L., Knippertz, P., Marsham, J.H. & Parker, D.J. (2015) The West African monsoon onset: a concise comparison of definitions. *Journal of Climate*, 28(22), 8673–8694. Available from: <https://doi.org/10.1175/JCLI-D-15-0265.1>
- Funk, C., Fink, A.H., Harrison, L., Segele, Z., Endris, H.S., Galu, G. et al. (2023) Frequent but predictable droughts in East Africa driven by a Walker circulation intensification. *Earth’s Future*, 11, e2022EF003454. Available from: <https://doi.org/10.22541/essoar.167591084.49882754/v1>
- Funk, C., Peterson, P., Landsfeld, M., Pedreros, D., Verdin, J., Shukla, S. et al. (2015) The climate hazards infrared precipitation with stations—a new environmental record for monitoring extremes. *Scientific Data*, 2(1), 150066. Available from: <https://doi.org/10.1038/sdata.2015.66>
- Gbangou, T., Ludwig, F., van Slobbe, E., Hoang, L. & Kranjac-Berisavljevic, G. (2019) Seasonal variability and predictability of agro-meteorological indices: tailoring onset of rainy season estimation to meet farmers’ needs in Ghana. *Climate Services*, 14, 19–30. Available from: <https://doi.org/10.1016/j.cliser.2019.04.002>
- Global Agricultural Monitoring. (2019) Special report: Kenya long rains rapid crop assessment (updated September 24th, 2019)-KenyaReliefWeb. Available from: <https://reliefweb.int/report/kenya/special-report-kenya-long-rains-rapid-crop-assessment-updated-september-24th-2019>
- Gudoshava, M., Wainwright, C., Hirons, L., Endris, H.S., Segele, Z.T., Woolnough, S. et al. (2022a) Atmospheric and oceanic conditions associated with early and late onset for eastern Africa short rains. *International Journal of Climatology*, 42, 6562–6578. Available from: <https://doi.org/10.1002/joc.7627>
- Gudoshava, M., Wanzala, M., Thompson, E., Mwesigwa, J., Endris, H.S., Segele, Z. et al. (2022b) Application of real time S2S forecasts over eastern Africa in the co-production of climate services. *Climate Services*, 27, 100319. Available from: <https://doi.org/10.1016/j.cliser.2022.100319>
- Herrmann, S.M. & Mohr, K.I. (2011) A continental-scale classification of rainfall seasonality regimes in Africa based on gridded precipitation and land surface temperature products. *Journal of Applied Meteorology and Climatology*, 50(12), 2504–2513. Available from: <https://doi.org/10.1175/JAMC-D-11-024.1>
- Hirons, L. & Turner, A. (2018) The impact of Indian Ocean mean-state biases in climate models on the representation of the East African short rains. *Journal of Climate*, 31(16), 6611–6631. Available from: <https://doi.org/10.1175/JCLI-D-17-0804.1>
- Hirons, L., Thompson, E., Dione, C., Indasi, V.S., Kilavi, M., Nkiaka, E. et al. (2021) Using co-production to improve the appropriate use of sub-seasonal forecasts in Africa. *Climate Services*, 23, 100246. Available from: <https://doi.org/10.1016/j.cliser.2021.100246>
- Indeje, M., Semazzi, F.H.M. & Ogallo, L.J. (2000) ENSO signals in East African rainfall seasons. *International Journal of Climatology*, 20(1), 19–46. Available from: [https://doi.org/10.1002/\(SICI\)1097-0088\(200001\)20:1<19::AID-JOC449>3.0.CO;2-0](https://doi.org/10.1002/(SICI)1097-0088(200001)20:1<19::AID-JOC449>3.0.CO;2-0)
- Kijazi, A.L. & Reason, C.J.C. (2012) Intra-seasonal variability over the northeastern highlands of Tanzania. *International Journal of Climatology*, 32(6), 874–887. Available from: <https://doi.org/10.1002/joc.2315>
- Kilavi, M., MacLeod, D., Ambani, M., Robbins, J., Dankers, R., Graham, R. et al. (2018) Extreme rainfall and flooding over Central Kenya including Nairobi City during the long-rains season 2018: causes, predictability, and potential for early warning and actions. *Atmosphere*, 9(12), 12. Available from: <https://doi.org/10.3390/atmos9120472>

- Kimani, M.W., Hoedjes, J.C.B. & Su, Z. (2017) An assessment of satellite-derived rainfall products relative to ground observations over East Africa. *Remote Sensing*, 9(5), 5. Available from: <https://doi.org/10.3390/rs9050430>
- Laux, P., Kunstmann, H. & Bárdossy, A. (2008) Predicting the regional onset of the rainy season in West Africa. *International Journal of Climatology*, 28(3), 329–342. Available from: <https://doi.org/10.1002/joc.1542>
- Liebmann, B. & Marengo, J. (2001) Interannual variability of the rainy season and rainfall in the Brazilian Amazon basin. *Journal of Climate*, 14(22), 4308–4318. Available from: [https://doi.org/10.1175/1520-0442\(2001\)014<4308:IVOTRS>2.0.CO;2](https://doi.org/10.1175/1520-0442(2001)014<4308:IVOTRS>2.0.CO;2)
- Liebmann, B., Bladé, I., Funk, C., Allured, D., Quan, X.-W., Hoerling, M. et al. (2017) Climatology and interannual variability of boreal spring wet season precipitation in the eastern Horn of Africa and implications for its recent decline. *Journal of Climate*, 30(10), 3867–3886. Available from: <https://doi.org/10.1175/JCLI-D-16-0452.1>
- MacLeod, D. (2018) Seasonal predictability of onset and cessation of the East African rains. *Weather and Climate Extremes*, 21, 27–35. Available from: <https://doi.org/10.1016/j.wace.2018.05.003>
- MacLeod, D.A., Dankers, R., Graham, R., Guigma, K., Jenkins, L., Todd, M.C. et al. (2021) Drivers and subseasonal predictability of heavy rainfall in equatorial East Africa and relationship with flood risk. *Journal of Hydrometeorology*, 22(4), 887–903. Available from: <https://doi.org/10.1175/JHM-D-20-0211.1>
- Marchant, R., Mumbi, C., Behera, S. & Yamagata, T. (2007) The Indian Ocean dipole—the unsung driver of climatic variability in East Africa. *African Journal of Ecology*, 45(1), 4–16. Available from: <https://doi.org/10.1111/j.1365-2028.2006.00707.x>
- Marteau, R., Moron, V. & Philippon, N. (2009) Spatial coherence of monsoon onset over Western and Central Sahel (1950–2000). *Journal of Climate*, 22(5), 1313–1324. Available from: <https://doi.org/10.1175/2008JCLI2383.1>
- Maybee, B., Ward, N., Hirons, L.C. & Marsham, J.H. (2022) Importance of Madden–Julian oscillation phase to the interannual variability of East African rainfall. *Atmospheric Science Letters*, 24, e1148. Available from: <https://doi.org/10.1002/asl.1148>
- Muita, R., Dougill, A., Mutemi, J., Aura, S., Graham, R., Awolala, D. et al. (2021) Understanding the role of user needs and perceptions related to sub-seasonal and seasonal forecasts on Farmers' decisions in Kenya: a systematic review. *Frontiers in Climate*, 3, 10. Available from: <https://doi.org/10.3389/fclim.2021.580556>
- Mutai, C., Polzin, D. & Hastenrath, S. (2012) Diagnosing Kenya rainfall in boreal autumn: further exploration. *Journal of Climate*, 25(12), 4323–4329. Available from: <https://doi.org/10.1175/JCLI-D-11-00414.1>
- Mutai, C.C. & Ward, M.N. (2000) East African rainfall and the tropical circulation/convection on intraseasonal to interannual timescales. *Journal of Climate*, 13(22), 3915–3939. Available from: [https://doi.org/10.1175/1520-0442\(2000\)013<3915:EARATT>2.0.CO;2](https://doi.org/10.1175/1520-0442(2000)013<3915:EARATT>2.0.CO;2)
- Mwangi, E., Taylor, O., Todd, M.C., Visman, E., Kniveton, D., Kilavi, M. et al. (2022) Mainstreaming forecast based action into national disaster risk management systems: experience from drought risk management in Kenya. *Climate and Development*, 14(8), 741–756. Available from: <https://doi.org/10.1080/17565529.2021.1984194>
- Kadi, M., Njau, L.N., Mwikya, J. & Kamga, A. (2011) *The state of climate information services for agriculture and food security in East African countries*. Copenhagen, Denmark: CGIAR Research Program on Climate Change, Agriculture and Food Security. Working paper 5. Available from: <https://cgspace.cgiar.org/handle/10568/6575>
- Nicholson, S.E. (2017) Climate and climatic variability of rainfall over eastern Africa. *Reviews of Geophysics*, 55(3), 590–635. Available from: <https://doi.org/10.1002/2016RG000544>
- Ogalló, L.J. (1988) Relationships between seasonal rainfall in East Africa and the Southern Oscillation. *Journal of Climatology*, 8(1), 31–43. Available from: <https://doi.org/10.1002/joc.3370080104>
- Omonge, P., Feigl, M., Olang, L., Schulz, K. & Herrnegger, M. (2022) Evaluation of satellite precipitation products for water allocation studies in the Sio-Malaba-Malakisi river basin of East Africa. *Journal of Hydrology: Regional Studies*, 39, 100983. Available from: <https://doi.org/10.1016/j.ejrh.2021.100983>
- Owusu, A., Tesfamariam Tekeste, Y., Ambani, M., Zebiak, S.E. & Thomson, M.C. (2017) *Climate Services for Resilient Development (CSRD) technical exchange in eastern Africa*. New York, NY: Climate Services for Resilient Development (CSRD). Workshop report. Available from: <https://cgspace.cgiar.org/handle/10568/89140>
- Palmer, P.I., Wainwright, C.M., Dong, B., Maidment, R.I., Wheeler, K.G., Gedney, N. et al. (2023) Drivers and impacts of eastern African rainfall variability. *Nature Reviews Earth & Environment*, 4, 254–270. Available from: <https://doi.org/10.1038/s43017-023-00397-x>
- Pohl, B. & Camberlin, P. (2006) Influence of the Madden–Julian Oscillation on East African rainfall. I: Intraseasonal variability and regional dependency. *Quarterly Journal of the Royal Meteorological Society*, 132(621), 2521–2539. Available from: <https://doi.org/10.1256/qj.05.104>
- Reynolds, R.W., Rayner, N.A., Smith, T.M., Stokes, D.C. & Wang, W. (2002) An improved in situ and satellite SST analysis for climate. *Journal of Climate*, 15, 1609–1625. Available from: [https://doi.org/10.1175/1520-0442\(2002\)015<1609:AIISAS>2.0.CO;2](https://doi.org/10.1175/1520-0442(2002)015<1609:AIISAS>2.0.CO;2)
- Saji, N.H., Goswami, B.N., Vinayachandran, P.N. & Yamagata, T. (1999) A dipole mode in the tropical Indian Ocean. *Nature*, 401, 360–363.
- Stern, R.D., Dennett, M.D. & Garbutt, D.J. (1981) The start of the rains in West Africa. *Journal of Climatology*, 1(1), 59–68. Available from: <https://doi.org/10.1002/joc.3370010107>
- UK Met Office. (2011) Climate Science Research Partnership (CSR/P): overview. Available from: [https://assets.publishing.service.gov.uk/media/57a08a85ed915d622c0007a3/60736-CSR/P\\_COLLECTED\\_Nov.pdf](https://assets.publishing.service.gov.uk/media/57a08a85ed915d622c0007a3/60736-CSR/P_COLLECTED_Nov.pdf)
- United States Department of Agriculture. (2009) Kenya's grain basket. Available from: <https://ipad.fas.usda.gov/highlights/2009/12/kenya/KenyasGrainBasket.htm>
- Vellinga, M. & Milton, S.F. (2018) Drivers of interannual variability of the East African “long rains”. *Quarterly Journal of the Royal Meteorological Society*, 144(712), 861–876. Available from: <https://doi.org/10.1002/qj.3263>
- Vellinga, M., Arribas, A. & Graham, R. (2013) Seasonal forecasts for regional onset of the West African monsoon. *Climate Dynamics*, 40(11–12), 3047–3070. Available from: <https://doi.org/10.1007/s00382-012-1520-z>

- Wainwright, C.M., Marsham, J.H., Keane, R.J., Rowell, D.P., Finney, D.L., Black, E. et al. (2019) "Eastern African Paradox" rainfall decline due to shorter not less intense long rains. *npj Climate and Atmospheric Science*, 2(1), 34. Available from: <https://doi.org/10.1038/s41612-019-0091-7>
- Walker, D.P., Birch, C.E., Marsham, J.H., Scaife, A.A., Graham, R.J. & Segele, Z.T. (2019) Skill of dynamical and GHACOF consensus seasonal forecasts of East African rainfall. *Climate Dynamics*, 53(7–8), 4911–4935. Available from: <https://doi.org/10.1007/s00382-019-04835-9>
- Wheeler, M.C. & Hendon, H.H. (2004) An all-season real-time multivariate MJO index: development of an index for monitoring and prediction. *Monthly Weather Review*, 132(16), 1932.
- White, C.J., Domeisen, D.I.V., Acharya, N., Adefisan, E.A., Anderson, M.L., Aura, S. et al. (2022) Advances in the application and utility of subseasonal-to-seasonal predictions. *Bulletin of the American Meteorological Society*, 103(6), E1448–E1472. Available from: <https://doi.org/10.1175/BAMS-D-20-0224.1>
- Young, M., Heinrich, V., Black, E. & Asfaw, D. (2020) Optimal spatial scales for seasonal forecasts over Africa. *Environmental*

*Research Letters*, 15(9), 094023. Available from: <https://doi.org/10.1088/1748-9326/ab94e9>

Zaitchik, B.F. (2017) Madden–Julian Oscillation impacts on tropical African precipitation. *Atmospheric Research*, 184, 88–102. Available from: <https://doi.org/10.1016/j.atmosres.2016.10.002>

## SUPPORTING INFORMATION

Additional supporting information can be found online in the Supporting Information section at the end of this article.

**How to cite this article:** Mwangi, E., MacLeod, D., Kniveton, D., & Todd, M. C. (2024). Variability of rainy season onsets over East Africa. *International Journal of Climatology*, 44(10), 3357–3379. <https://doi.org/10.1002/joc.8528>